# The Capacity to Act in *Trans* Varies Among *Drosophila* Enhancers

Amanda J. Blick,[1] Ilana Mayer-Hirshfeld,[1] Beatriz R. Malibiran, Matthew A. Cooper, Pieter A. Martino,
Justine E. Johnson, and Jack R. Bateman[2]

Biology Department, Bowdoin College, Brunswick, Maine 04011

**ABSTRACT** The interphase nucleus is organized such that genomic segments interact in *cis*, on the same chromosome, and in *trans*, between different chromosomes. In *Drosophila* and other Dipterans, extensive interactions are observed between homologous chromosomes, which can permit enhancers and promoters to communicate in *trans*. Enhancer action in *trans* has been observed for a handful of genes in *Drosophila*, but it is as yet unclear whether this is a general property of all enhancers or specific to a few. Here, we test a collection of well-characterized enhancers for the capacity to act in *trans*. Specifically, we tested 18 enhancers that are active in either the eye or wing disc of third instar *Drosophila* larvae and, using two different assays, found evidence that each enhancer can act in *trans*. However, the degree to which *trans*-action was supported varied greatly between enhancers. Quantitative analysis of enhancer activity supports a model wherein an enhancer's strength of transcriptional activation is a major determinant of its ability to act in *trans*, but that additional factors may also contribute to an enhancer's *trans*-activity. In sum, our data suggest that a capacity to activate a promoter on a paired chromosome is common among *Drosophila* enhancers.

**KEYWORDS** RMCE; interchromosomal interactions; long-range enhancer; somatic homolog pairing; transvection

**T**HE spatial organization of the interphase eukaryotic genome is characterized by extensive long-distance interactions between distal chromosome regions (Sanyal *et al.* 2012). Interactions have been identified between sequences on the same chromosome (in *cis*) or on different chromosomes (in *trans*) (Lieberman-Aiden *et al.* 2009; Duan *et al.* 2010; Sexton *et al.* 2012; van de Werken *et al.* 2012; Nagano *et al.* 2013; Zhang *et al.* 2013). Many long-distance interactions in *cis* underlie the activation of specific genes, and in some cases, sequences have been identified that facilitate interactions between a distal enhancer and a specific promoter target (Zhou and Levine 1999; Calhoun *et al.* 2002; Calhoun and Levine 2003; Lin 2003; Akbari *et al.* 2008; Fujioka *et al.* 2009; Majumder *et al.* 2015). In contrast, the genetic impacts of *trans*-interactions between chromosomes are less clearly understood. Examples of

gene regulation involving interchromosomal associations have been described (Spilianakis *et al.* 2005; Bacher *et al.* 2006; Xu *et al.* 2006; Apostolou and Thanos 2008; Sandhu *et al.* 2009; Markenscoff-Papadimitriou *et al.* 2014; Patel *et al.* 2014), but it remains unclear whether it is common for sequences that regulate gene expression to communicate between different chromosomes when they are physically juxtaposed.

In *Drosophila melanogaster*, extensive *trans*-interactions are observed between homologous chromosomes in virtually all somatic tissues, a phenomenon known as somatic homolog pairing (reviewed by McKee 2004; Bosco 2012). The close proximity of homologous chromosomes in *Drosophila* can permit an enhancer to act in *trans* on a promoter on the paired homolog, a form of pairing-dependent gene regulation called transvection (Lewis 1954). Evidence for enhancer action in *trans* has been uncovered at a handful of genes in the *Drosophila* genome, often providing an explanation for unexpected intragenic complementation of loss-of-function alleles (Lewis 1954; Gelbart 1982; Geyer *et al.* 1990; Leiserson *et al.* 1994; Hendrickson and Sakonju 1995; Casares *et al.* 1997; Morris *et al.* 1998; Southworth and Kennison 2002; Marin *et al.* 2004; Coulthard *et al.* 2005; Gohl *et al.* 2008; Juni and Yamamoto 2009), or the nonadditive activity of

paired mutant and wild-type alleles (Gibson *et al.* 2000; Lum and Merritt 2011; Bing *et al.* 2014).

More recently, transgenic approaches based on site-specific recombination have been developed for *Drosophila* to query specific enhancer fragments and genomic positions for support of transvection (Chen *et al.* 2002; Kravchenko *et al.* 2005; Bateman *et al.* 2012a; Mellert and Truman 2012; also see Kassis *et al.* 1991). Thus far, transvection has been observed at all genomic insertion sites tested, suggesting that the *Drosophila* genome is generally permissive to enhancer action in *trans*. Furthermore, transgenic experiments have demonstrated that promoters at allelic positions in *cis* and *trans* to an enhancer will compete for the enhancer's activity, consistent with earlier classical observations (Geyer *et al.* 1990; Martinez-Laborda *et al.* 1992; Casares *et al.* 1997; Morris *et al.* 1999; Gohl *et al.* 2008). However, enhancer activation of promoters in *cis* and *trans* are not equivalent, with enhancers showing a strong preference for a promoter in *cis*, and frequently showing cell-to-cell variability in the activation of a promoter in *trans* (Bateman *et al.* 2012a; Mellert and Truman 2012).

Recently, Mellert and Truman (2012) used a transgenic approach to test 21 *Drosophila* enhancers for the capacity to support transvection. Their assay provided evidence that some, but not all, tested enhancers could activate a promoter on a paired homolog, raising the question of whether the capacity to act in *trans* is special to some enhancers. It does not appear that specific "tethering" sequences are required for an enhancer to act in *trans* since minimal enhancers consisting of multimerized binding sites for a single transcription factor can function in *trans*, even when that transcription factor is not native to *Drosophila* (Bateman *et al.* 2012a; Mellert and Truman 2012). Notably, in the system employed by Mellert and Truman, enhancers were generally juxtaposed to a strong promoter in *cis*, which may have decreased the likelihood of observing enhancer action in *trans*. Thus, their analysis may represent an underestimate of the proportion of enhancers that can support transvection.

Here we assess the generality of enhancer action in *trans* by testing a collection of known *Drosophila* enhancers for the capacity to support transvection. We employed a transgenic system that placed a weak, or absent, promoter in *cis* and a fluorescent reporter in *trans* to a collection of enhancers that act in third instar larval discs, tissues known to support transvection. Our data show evidence for enhancer action in *trans* for all enhancers tested, implying that the capacity to support transvection is a common property shared by *Drosophila* enhancers.

## Materials and Methods

### Stocks and fly husbandry

Flies carrying an enhancerless *GFP* construct downstream of an *hsp70* minimal promoter at recombinase-mediated cassette exchange (*RMCE*) site 53F were described pre-

viously (Bateman *et al.* 2012a). Flies of genotype w[*]; *P[w[+mC]=Ubi-p63E(FRT.STOP)Stinger]15F2* (Evans *et al.* 2009), carrying an FRT-flanked stop cassette between a ubiquitous promoter and a nuclear *EGFP* coding region on chromosome 3 ("G-TRACE cassette"), were obtained from the Bloomington *Drosophila* Stock Center (stock no. 32251). All flies were maintained at 25° on standard *Drosophila* cornmeal, yeast, sugar, and agar medium with p-hydroxybenzoic acid methyl ester as a mold inhibitor.

### Plasmid construction and transgenics

Construction of piB-LTL-lacZ, an RMCE donor vector with loxP sites flanking an *hsp70* minimal promoter upstream of a *lacZ* coding region, and GMR-LTL-lacZ, was described previously (Bateman *et al.* 2012a). To generate piB-LTL-lacZ derivatives carrying different enhancers, potential target enhancers were identified using the REDFly database (Gallo *et al.* 2011), and primers for amplifying enhancer sequences were either identified from a previous publication (Aerts *et al.* 2010) or designed using Primer3 software (Untergasser *et al.* 2012). Enhancer sequences were amplified via PCR from *Drosophila* genomic DNA and cloned into either pcr2.1 using a TOPO-TA cloning kit (Invitrogen) or pSC-A using a Strataclone PCR cloning kit (Agilent Technologies). Subcloned fragments were digested from these vectors and cloned into piB-LTL-lacZ using *Bam*HI. Primer sequences for amplifying enhancers are listed in Supplemental Material, Table S1.

An RMCE donor vector carrying the *hsp70* minimal promoter upstream of a *FLP* coding region was generated via a PCR-based strategy (Bateman and Wu 2008) using the template pCaSpeR-DEST5 (obtained from the *Drosophila* Genomics Resource Center) and primers hsp70FLP_5_attB40 and hsp70FLP_3_attB40 (additional primer sequences are provided in Table S2). The final donor vector was created by cloning the resulting PCR product into pSC-A using a Strataclone PCR cloning kit.

*Paxpaxpax-LTL-lacZ* and *salsalsal-LTL-lacZ,* carrying three tandem copies of the *pax* and *sal* enhancers, respectively, were created by serial cloning of PCR-amplified enhancer fragments with primer-encoded restriction sites into piB-LTL-lacZ. Briefly, a PCR fragment carrying the enhancer, a single *Xho*I site, and flanked by *Bam*HI sites, was cloned into a *Bam*HI site upstream of the promoter of piB-LTL-lacZ. Next, a second fragment carrying the same enhancer with a single *Stu*I site and flanked by *Xho*I sites was cloned into the *Xho*I site created in the previous step. Finally, a third fragment carrying the enhancer flanked by *Stu*I sites was cloned into the new *Stu*I site.

All donor constructs were integrated into an RMCE target site at position 53F via RMCE as previously described (Bateman *et al.* 2006, 2012a; Bateman and Wu 2008). Following integration, the orientation of each insert was assessed using primers lac4 or 3′-Pend1, which are complementary to the 5′ and 3′ *P*-element ends flanking the RMCE cassette, respectively, and RNXG9, which is complementary to the SV40 3′-UTR downstream of the *lacZ* and

*FLP* coding regions. All constructs were analyzed using insertions oriented with the 3′-UTR closest to the 5′ *P*-element end, with the exception of *CG1625-LTL-lacZ*, for which only one insertion in the opposite orientation was obtained. Promoterless derivatives of *pax-LTL-lacZ* and *klu-LTL-lacZ* insertions were generated via Cre/loxP recombination as previously described (Siegal and Hartl 1996; Bateman *et al.* 2012a).

### Staining and microscopy

Imaginal discs were dissected from wandering third instar larvae in phosphate-buffered saline (PBS) and fixed in 4% formaldehyde (Electron Microscopy Sciences) in PBS for 20 min. Discs were then rinsed three times in PBS plus 0.1% Triton X-100 (PBST) and blocked in 4% normal goat serum (NGS) in PBST for 1 hr, then incubated with primary antibodies overnight at 4°. Antibodies used were polyclonal rabbit anti-GFP (1:2000; Invitrogen), mouse monoclonal antibodies elav-9F8A9 (Elav), 2B10 (Cut), and 40-1a (β-galactosidase, β-gal) (1:400, 1:100, 1:110, respectively; Developmental Studies Hybridoma Bank, DSHB), and rat monoclonal antibody Rat-Elav-7E8A10 (1:250; DSHB). Next, discs were rinsed and then washed two times for 20 min each in PBST, blocked in 4% NGS/PBST for 1 hr, and then incubated for 1 hr with secondary antibodies antirabbit Alexa Fluor-488 (1:2000; Invitrogen), antimouse-Cy3 (1:250; Jackson Immunoresearch), antirat-Cy3 (1:250; Jackson), and/or antimouse-Cy5 (1:250; Jackson) as required. Discs were then washed four times for 20 min each in PBST and mounted in Fluoromount G with DAPI (Affymetrix eBioscience). Discs were imaged using a Zeiss Axio Imager.A2 fluorescence microscope with an AxioCam MRm camera and Zen software. Confocal imaging was performed using a Zeiss Axioplan 2 microscope with a 510 Meta confocal laser scanning system. Statistical analyses were performed using Prism (GraphPad Software) or R Statistical Software packages. A D'Agostino and Pearson omnibus normality test was used to determine whether to test data via parametric or nonparametric methods.

To stain for β-galactosidase activity, imaginal discs were dissected from wandering third instar larvae in PBS, fixed for 15 min in 1% glutaraldehyde/PBS, rinsed three times in PBST, and then incubated in X-gal staining solution [10 mM $NaH_2PO_4$ pH 7.2, 150 mM NaCl, 3.3 mM $K_3[Fe(CN)_6]$, 3.3 mM $K_4[Fe(CN)_6]$, 0.1% Tween, 0.2% X-gal] at room temperature. Following staining, discs were rinsed three times in PBST and then mounted in 80% glycerol. Discs were imaged using an Olympus BX51 compound microscope equipped with a Media Cybernetics Evolution VF color camera and QCapture Pro Software.

### Quantitative RT-PCR

Assessment of mRNA levels via quantitative RT-PCR was performed as previously described (Bateman *et al.* 2012a). Briefly, for each sample, 20 imaginal discs were dissected from wandering third instar larvae and frozen at −80°.

Tissue homogenization, genomic DNA elimination, and RNA purification were carried out using an RNeasy plus kit (Qiagen) according to the manufacturer's protocol. PCR was performed on a StepOne Real-Time PCR system (Applied Biosystems) using cDNA diluted 1:5 into SYBR green PCR Mastermix (Applied Biosystems). Primers SV40_3′-UTR_2F and SV40_3′-UTR_2R were used to amplify lacZ cDNA, and RP49-58F and RP49-175R were used to amplify the housekeeping rp49 cDNA as an internal reference. Relative levels of transcript were calculated via the ΔΔCt method using StepOne software.

### Data availability

The authors state that all data necessary for confirming the conclusions presented in the article are represented fully within the article.

## Results

To test whether the capacity to act in *trans* is a common property of *Drosophila* enhancers, we designed a transgene-based strategy using *lacZ* and *GFP* reporters. Since some enhancers were previously shown to have decreased action in *trans* in the presence of a promoter in *cis*, the *lacZ* reporter was designed to permit removal of its *hsp70* promoter via Cre/loxP recombination [designated the "loxP-TATA-loxP" (LTL) promoter] (Figure 1). The reporter construct also carried attB sequences suitable for RMCE, permitting targeted transgene insertion in the absence of phenotypic markers (Bateman *et al.* 2006). Our strategy was to clone various enhancers into the reporter, then target each construct to a common location in the *Drosophila* genome where an enhancerless *hsp70-GFP* reporter had already been placed. The activity of each enhancer in *cis* can then be assessed by β-gal activity, while *trans*-action can be determined by GFP fluorescence (Figure 1).

We first tested the eye-specific enhancer *GMR*, which was previously shown to support transvection in the developing larval eye disc (Bateman *et al.* 2012a). In comparison to a *GMR-hsp70-lacZ* transgene lacking loxP sites, β-galactosidase activity from the *GMR-LTL-lacZ* reporter was substantially weaker, with an ~40-fold difference in *lacZ* transcript levels as assessed by quantitative RT-PCR (Figure S1). We did not further pursue the nature of the decreased activity, possibly caused by interference of the loxP sites with the function of the promoter, but we reasoned that the weak action of the LTL promoter should be advantageous to our analysis of transvection since a weak promoter in *cis* is more likely to release an enhancer's activity to a strong promoter in *trans* (Morris *et al.* 1999; Mellert and Truman 2012). Importantly, *GMR-LTL-lacZ* activation of *GFP* in *trans* was observed in the expected pattern in cells posterior to the morphogenetic furrow of third instar eye discs (Figure 1B and Figure 2), demonstrating that this system supports enhancer action in *trans*.

We then selected an additional 14 enhancers from the REDfly database of known *Drosophila cis* regulatory elements (Gallo *et al.* 2011) (Table 1). We focused on enhancers that
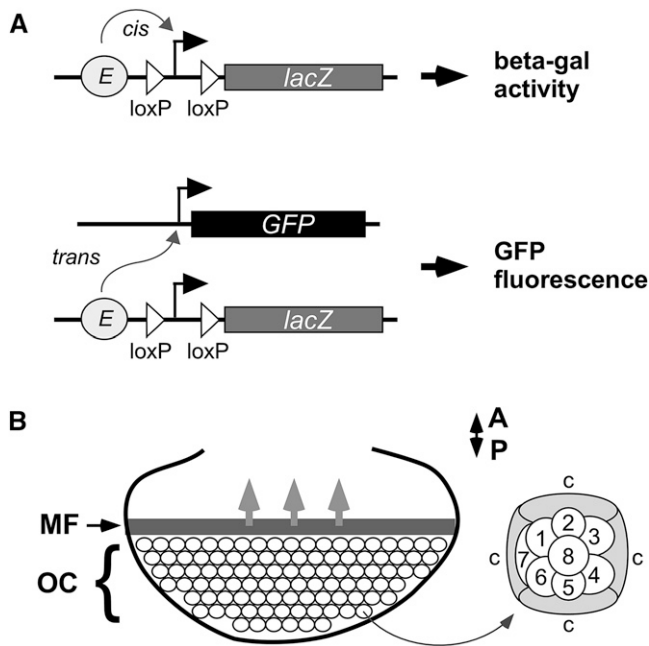
**Figure 1** Study strategy. (A) Each enhancer is cloned into a common reporter carrying a minimal *hsp70* promoter flanked by loxP sites and upstream of a *lacZ* coding region. Enhancer activation of the promoter in *cis* can be assessed by staining for β-gal activity. Enhancer action in *trans* is assessed by placing each *lacZ* construct in *trans* to an enhancerless *hsp70-GFP* construct at the same genomic location and assessing GFP fluorescence. Note that the promoter of the *lacZ* construct can also be removed by Cre/loxP-mediated recombination. (B) Cartoon representation of a third instar eye disc. The morphogenetic furrow (MF) represents a wave of mitotic divisions that moves from the posterior (down) to the anterior (up) of the disc. Cells anterior to the MF are precursor cells that have not yet differentiated, while those posterior to the MF initiate a pattern of differentiation to form ommatidial clusters (OC). Each mature cluster consists of eight photoreceptor cells, R1–R8, surrounded by four cone cells (c), all of which develop via a stereotyped developmental program following the passage of the MF. OC schematic is adapted from Mavromatakis and Tomlinson (2013).

are active in stereotyped patterns across the developing ommatidial clusters of the third instar larval eye disc, reasoning that this tissue is generally permissive to transvection based on prior analyses (Leiserson *et al.* 1994; Wu and Howe 1995; Bateman *et al.* 2012a). Each enhancer was cloned upstream of the *LTL-lacZ* construct, targeted to a common RMCE site and crossed to flies carrying the enhancerless *hsp70-GFP* at the same genomic location. As a negative control, we also assayed a wing disc-specific enhancer fragment from the gene *sal* (Guss *et al.* 2001).

In third instar eye discs carrying the *sal* wing enhancer, we observed only a low level of background autofluorescence distributed evenly across the tissue (Figure 2). In contrast, for all 14 eye-specific enhancers, we observed cells with green fluorescence above background levels, consistent with each enhancer having some capacity to activate a promoter in *trans*. In all cases, the pattern of fluorescence was unevenly distributed across the regularly patterned ommatidial clusters, consistent with the variegated pattern of transvection

previously observed for *GMR* in this tissue (Bateman *et al.* 2012a) (Figure 2). The levels of GFP fluorescence and numbers of GFP-positive cells varied greatly for the different enhancers, with some enhancers showing broad GFP fluorescence across the tissue, while others showed just a few fluorescent cells in some, but not all, discs. We qualitatively assigned each enhancer to one of three general classes of transvection strength: strong, with many GFP-positive cells present in all discs (four enhancers, including *GMR*), moderate, with fewer scattered GFP-positive cells present in all discs (three enhancers), and weak, with some discs showing a few GFP-positive cells and others showing none (eight enhancers). For two enhancers of the weak class, *pax* and *klu*, we used Cre/loxP-mediated recombination to remove the promoter in *cis* to the enhancer and then repeated the analysis of transvection. In the case of the *klu* enhancer, the proportion of discs showing GFP-positive cells increased significantly (3/9 *vs.* 16/20, *P* = 0.03, Fisher's exact test), whereas no significant change was observed for the *pax* enhancer (12/20 *vs.* 7/11, *P* = 1.0), suggesting that enhancers may differ in sensitivity to a weak promoter in *cis*. Given the weak nature of the *LTL* promoter and the widespread enhancer action in *trans* observed in its presence, we did not pursue removal of the promoter for other enhancer constructs. In sum, our analysis suggests that the capacity to act in *trans* is a general property of enhancers acting in the eye disc, but the strength with which they do so varies greatly.

### A FLP-based assay further supports transvection by weak class enhancers

Although the enhancers of the weak class each showed evidence of transvection when placed in *trans* to *hsp70-GFP*, the GFP fluorescence was frequently at our limit of detection using fluorescence microscopy. We therefore wished to provide further confirmation that these enhancers indeed activate promoters in *trans*. To this end, we designed a complementary system to detect transvection based on the G-TRACE tools for cell lineage analysis (Evans *et al.* 2009). In this system, the recombinase FLP acts on a G-TRACE cassette to remove a transcriptional stop signal between a ubiquitous enhancer and a *GFP* transgene, resulting in robust GFP fluorescence in a cell's lineage (Figure 3A). To adapt G-TRACE to the study of transvection, we targeted an *hsp70-FLP* construct to RMCE site 53F so that it could be placed in *trans* to enhancers of the weak transvection class. We reasoned that this scheme would result in a highly sensitive detection method; indeed, in negative control discs carrying the G-TRACE cassette in which an enhancerless *hsp70-lacZ* was placed in *trans* to *hsp70-FLP*, we observed an occasional GFP-positive cell posterior to the morphogenetic furrow, suggesting that the level of background activity of the *hsp70-FLP* construct in the absence of an enhancer is very close to the threshold level required for removal of the transcriptional stop signal of the G-TRACE cassette.

We crossed flies carrying each *enhancer-LTL-lacZ* construct of the weak transvection class to flies carrying *hsp70-FLP* and
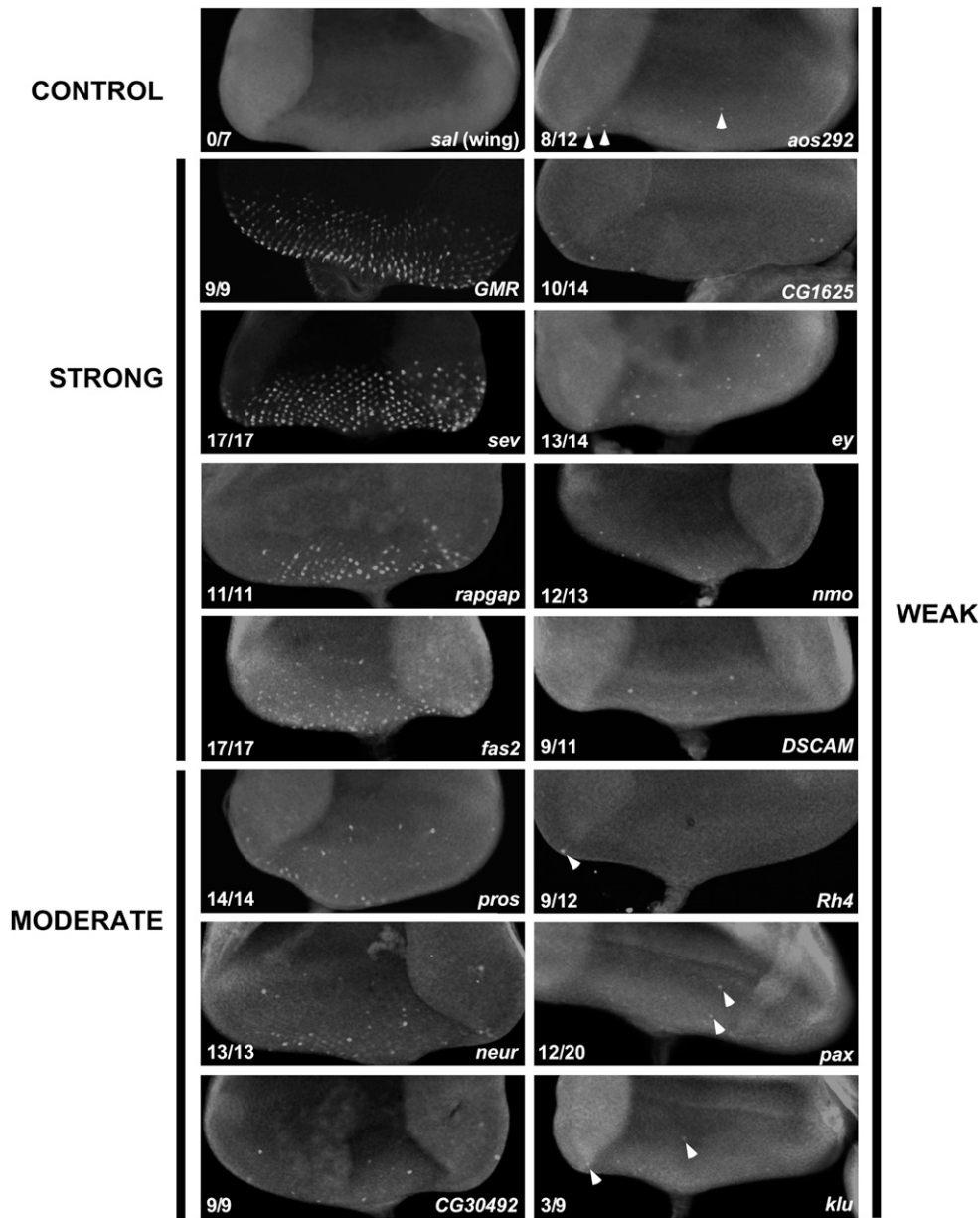
**Figure 2** Enhancers active in the third instar eye disc act in *trans* with varying strengths. Each panel shows a representative eye disc carrying the indicated enhancer in *trans* to *hsp70-GFP*, with the fraction of scored discs that show GFP-positive cells indicated. The wing-specific enhancer *sal* was used as a negative control. Each enhancer was qualitatively assigned to a strong, moderate, or weak transvection class based on the number of GFP-positive cells observed (see main text). Arrowheads indicate weak GFP-positive cells.

the G-TRACE cassette and scored the number of GFP-positive cells in each eye disc for at least 10 discs of each genotype (with the exception of *ey*; see below). For each enhancer, the mean number of GFP-positive cells was significantly higher than that of negative control discs lacking an enhancer (adjusted $P < 0.05$ for each enhancer, Kruskal–Wallis test with Dunn's multiple comparisons test) (Figure 3, B and C), further supporting that each enhancer has the capacity to activate a promoter in *trans*. Notably, this analysis confirmed that the enhancer *Rh4* supports transvection in the larval eye disc, an unexpected result given that the *Rh4* gene is normally active later in development (see *Discussion*).

The weak class enhancers analyzed above are active in postmitotic cells, which are not expected to undergo cell divisions once GFP has been activated. In contrast, the weak class enhancer *ey* becomes active in eye-specific precursor

cells during embryogenesis (Halder *et al.* 1998; Hauck *et al.* 1999), allowing us to use the G-TRACE system to determine the stage(s) at which this enhancer can act in *trans*; if transvection by the *ey* enhancer is restricted to postmitotic cells, we should only observe single GFP-positive cells posterior to the morphogenetic furrow, whereas if the enhancer acts in *trans* before this time, we should see clonal patches of GFP-positive cells. Analysis of the *ey* enhancer showed evidence of both of these predictions: among differentiated cells, some single GFP-positive cells were surrounded by nonfluorescent neighboring cells, whereas in other areas of the disc, larger clusters of GFP-positive cells were observed (Figure 4). Note that clonal patches of GFP-positive cells were also observed anterior to the furrow, consistent with the early action of the *ey* enhancer (Figure S2). Importantly, clusters of fluorescent cells were never observed in negative control eye discs

**Table 1 Enhancers analyzed in this study**

| Enhancer name | Size (bp) | Cell-type specificity | Distance to promoter (kb) | Reference |
|---|---|---|---|---|
| aos | 292 | Cone cells | Intron, 6 | Wildonger et al. 2005 |
| CG1625 | 801 | Photoreceptor precursors | Upstream, 0 | Aerts et al. 2010 |
| CG30492 | 601 | Photoreceptor precursors | Upstream, 0 | Aerts et al. 2010 |
| dscam | 1703 | Photoreceptor precursors | Intron, 10 | Aerts et al. 2010 |
| ey | 212 | Eye primordial cells | Intron, 12 | Hauck et al. 1999 |
| fas2 | 539 | Photoreceptor precursors | Intron, 13 | Aerts et al. 2010 |
| GMR | 190 | Photoreceptors | Upstream, 0 | Moses and Rubin 1991 |
| klu | 364 | R1, R6, R7, cone cells | Intron, 10 | Wildonger et al. 2005 |
| neur | 809 | Photoreceptor precursors | Intron, 8–14 | Aerts et al. 2010 |
| nmo | 754 | Photoreceptor precursors | Intron, 50 | Aerts et al. 2010 |
| pax | 361 | Cone cells | Intron, 7 | Flores et al. 2000 |
| pros | 1220 | R3, R4, R7, cone cells | Intron, 32 | Xu et al. 2000 |
| Rapgap1 | 802 | Photoreceptor precursors | Intron, 1 | Aerts et al. 2010 |
| Rh4 | 159 | Photoreceptors | Upstream, 1 | Fortini and Rubin 1990 |
| sev | 476 | R3, R4, R7, cone cells[a] | Intron, 6 | Bowtell et al. 1991 |
| Ser | 812 | Wing margin | Downstream, 22 | Yan et al. 2004 |
| sal | 328 | Wing pouch quadrants | Upstream, 9 | Guss et al. 2001 |
| ct(2.7) | 2.7 kb | Wing margin, Air Sac Primordium (ASP) | Upstream, ~80 | Jack et al. 1991 |
| ct(668) | 668 | Wing margin | Upstream, ~80 | Guss et al. 2001 |

[a] Highest early expression in R3 and R4, with later high expression in R7 and cone cells. Reports conflict regarding weak expression in R1, R6, and mystery cells (Tomlinson et al. 1987; Bowtell et al. 1991; Domingos et al. 2004).

lacking an enhancer in *trans* to *hsp70-FLP* (*n* = 26) nor in discs carrying other weak class enhancers that are not active in embryonic precursor cells (*n* = 141). Among the discs analyzed, two large clonal patches created by the enhancer *ey*, likely derived from individual GFP-positive precursors, showed ~180–200 GFP-positive cells, suggesting that at least seven to eight cell cycles had passed since the activation of FLP led to removal of the stop signal in the G-TRACE cassette (Figure 4C). Thus, the enhancer *ey* has the capacity to act in *trans* early in the development of the eye.

### Cell-type specificity of transvection correlates with strength and timing of cis-activity

Among the enhancers analyzed, *GMR* and *sev* were the most consistent and robust activators of GFP in *trans*. In both cases, the majority of mature ommatidia appeared to have at least one GFP-positive cell (Figure 2). However, it was rare for more than one or two cells per ommatidium to be GFP positive, in contrast to the expected patterns of expression in *cis*, where each enhancer can act in multiple cell types within each ommatidial cluster (Table 1). To determine which cell types showed *GFP* expression in these discs, we used anti-Elav, a marker of neuronal photoreceptor cells. Specifically, anti-Elav highlights eight cells per mature cluster, R1–R8, each of which occupies a stereotyped position relative to the axes of the disc (Tomlinson et al. 1987; Bowtell et al. 1989) (Figure 1B). In discs where *GFP* was activated in *trans* by *GMR*, high-resolution confocal microscopy confirmed that most ommatidial clusters contained just one or two GFP-positive cells (Figure 5A). Based on their positions within the photoreceptor clusters, GFP-positive cells were most commonly either R3 (57% of ommatidia scored) or R4 (84%), with other cell types rarely showing GFP fluorescence (9%) (Table 2). We confirmed the strong bias of GFP-positive cells

to R3 and R4 using the marker *mδ0.5-lacZ*, which shows highest expression levels in R4 (Cooper and Bray 1999; Domingos et al. 2004) and occasional weak labeling of R3 in later ommatidia (Figure S3). This bias was not due to a position effect at 53F, as identical constructs inserted at a different genomic location showed a similar bias for R3 and R4 (data not shown). Importantly, all GFP-positive cells resulting from *GMR* transvection at 53F were also positive for Elav, indicating that *trans*-activation by the *GMR* enhancer was restricted to the expected cell types where *GMR* is known to act.

To further investigate the bias in transvection by *GMR*, we analyzed the relative strength of the enhancer in *cis* across different photoreceptor identities. At high resolution, expression of *lacZ* driven by the weak LTL promoter was patchy and inconsistent across the tissue, and therefore not suitable for quantitative imaging of single cells (data not shown). We therefore analyzed expression of an existing construct wherein *GFP* is driven in *cis* by *GMR* and an *hsp70* promoter lacking loxP sites (Bateman et al. 2012a). *GFP* expression was noticeably high in R3 and R4 in virtually all ommatidial clusters (Figure 5B; Figure S4); to quantify this pattern, we compared the fluorescence intensity of the R4 cell in each cluster to that of R2, representative of a cell type with low fluorescence, or R3, with fluorescence similar to that of R4. Averaged across 86 ommatidia, R4 was roughly twice as bright as R2 (mean relative intensity = 2.17 ± 0.55) but equivalent in intensity with R3 (mean relative intensity = 1.06 ± 0.26). Thus, a plausible explanation to account for cell-type bias in *GMR*-mediated transvection is that R3 and R4 show the highest level of *GMR* activity in *cis*, and therefore may have a higher probability of showing activation of a promoter in *trans*.

Similar to the case with *GMR*, *sev* expression in *cis* is highest in R3 and R4 in early ommatidial clusters, followed by later increases in expression in R7 and in cone cells
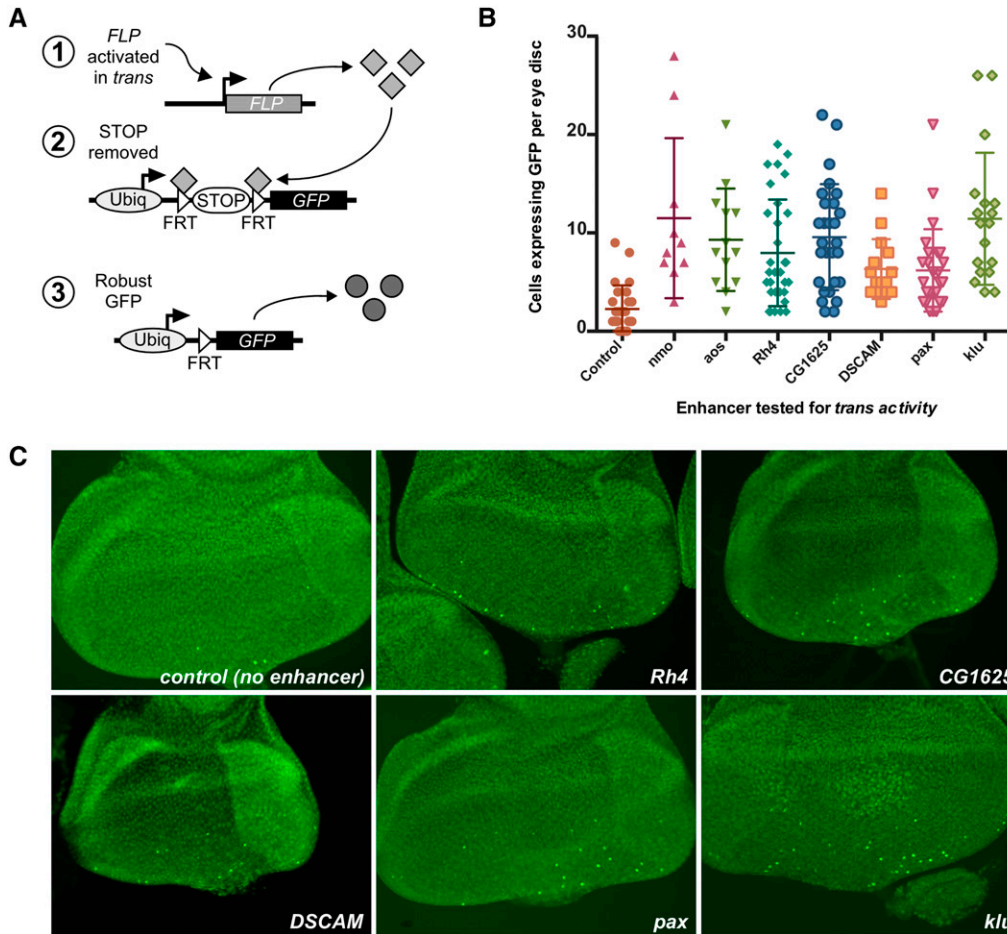
**Figure 3** G-TRACE-based strategy further supports enhancer action in *trans* by weak class enhancers. (A) Schematic for an alternative detection scheme, where *hsp70-GFP* (Figure 1A) is replaced with *hsp70-FLP*. *Trans*-activation of FLP at suitable levels removes a transcriptional stop signal on a G-TRACE cassette located at a different genomic location, resulting in strong GFP fluorescence in that cell. Schematic adapted from Evans *et al.* (2009). (B) Scoring of GFP-positive cells using the G-TRACE system. Each symbol represents the number of GFP-positive cells in a single disc; lines overlaying each cluster of symbols represent mean ± SD. (C) Representative eye discs from flies carrying the indicated enhancer activating the G-TRACE system (*nmo* and *aos* not shown).

(Tomlinson *et al.* 1987; Bowtell *et al.* 1989, 1991; Domingos *et al.* 2004). Notably, discs where *GFP* was activated in *trans* by *sev* once again showed a strong bias for R3 and R4 *vs.* other cells (Figure 5C; Table 2). Specifically, out of 203 ommatidia scored for transvection by *sev*, we observed only six cases of GFP-positive cells that were not R3 or R4; of those six, five were also positive for Elav, though we did not precisely determine their identities, and one was negative for Elav, with positioning and appearance consistent with a cone cell (data not shown). In contrast to *GMR* and *sev*, the strong class enhancer *fas2* has not been reported to show biased expression in subsets of photoreceptors (Aerts *et al.* 2010). In discs where *fas2* activates *GFP* in *trans*, GFP-positive cells were restricted to neuronal fates as expected, and the bias toward R3 and R4 was strongly reduced (Figure 5D; Table 2), consistent with a model wherein the cell-type-specific strength of enhancer action in *cis* is predictive of biased cell-type specificity of transvection. However, for all three strong class enhancers analyzed, *trans*-activation of GFP was always observed most often in R4, with the strongest bias observed for the *sev* enhancer and the mildest for *fas2*. Thus, while the strength and timing of an enhancer's activity may have a strong effect on the likelihood of transvection in a particular cell identity, other factors may also favor transvection in particular cell types.

We also attempted to determine cell-type specificity for GFP-positive cells resulting from weak class enhancers acting on *hsp70-GFP* in *trans*, but the GFP fluorescence produced by these genotypes was typically at the limit of detection and not sufficiently robust to confidently assign cell identities at high resolution. We therefore turned to our FLP-based assay, where GFP fluorescence produced by the G-TRACE cassette is strong and easily detected. However, analysis of this system was complicated by the low frequency spontaneous FLP activity in the absence of transvection (Figure 3). To better understand the spontaneous activity, we used either anti-Elav, a marker of neuronal photoreceptors, or anti-Cut, a marker of cone cells (Blochlinger *et al.* 1993), to costain control discs carrying the G-TRACE cassette wherein *hsp70-FLP* was placed in *trans* to an enhancerless *hsp70-lacZ* cassette. Our data indicate that the spontaneous activity is restricted to cells of neuronal fate, with complete overlap between GFP and Elav staining (23/23 cells from eight discs) and no overlap between GFP and Cut staining (0/19 cells from eight discs). We then analyzed discs carrying the G-TRACE cassette wherein *hsp70-FLP* was placed in *trans* to a cone-cell-specific enhancer, either *pax* or *aos* (Flores *et al.* 2000; Wildonger *et al.* 2005) and costained with anti-Cut, reasoning that any overlap between GFP and Cut staining must result from the activity of the enhancer and not from spontaneous FLP
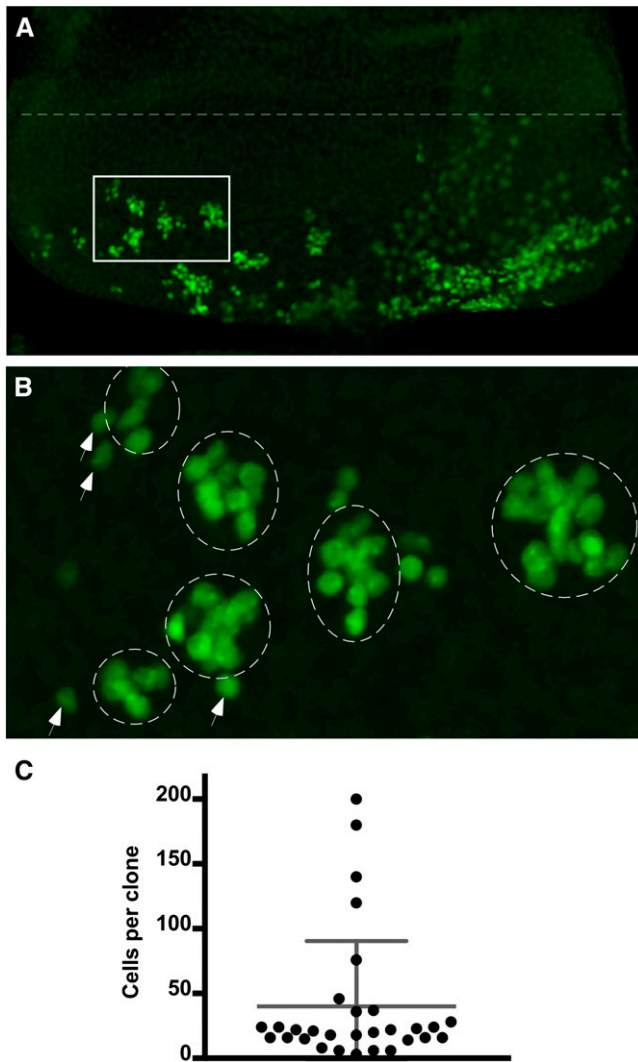
**Figure 4** The enhancer *ey* acts in *trans* early in development. (A) Eye disc with clonal regions of GFP-positive cells resulting from *trans*-activation of *hsp70-FLP* by the *ey* enhancer and subsequent activation of the G-TRACE cassette. Dashed line, morphogenetic furrow. (B) *Z*-projected confocal image of inset area from A. Clones (dashed circles) were defined as overlapping/touching groups of GFP-positive cells (>2) with no evidence of intervening GFP-negative cells. Single GFP-positive cells contacting only GFP-negative cells (arrows) were not scored. The region shown was scored as six clonal patches, with between 6 and 24 GFP-positive cells per clone. (C) The number of GFP-positive cells per clone was counted or estimated for 30 clonal patches. Overlaid lines represent mean ± SD.

activity on the G-TRACE cassette. In both cases, we saw colocalization between GFP and Cut staining that differed significantly from control discs (Figure S5). Specifically, for *aos*-mediated transvection using the G-TRACE system, 32/34 GFP-positive cells were also positive for Cut, whereas *pax* transvection led to fewer total numbers of GFP-positive cells, 9/45 of which were positive for Cut. Although we cannot exclude the possibility that weak class enhancers activate GFP outside their expected cell types (see *Discussion*), our data are consistent with transvection by *pax* and *aos* enhancers being primarily restricted to cone cells.

## Enhancer transvection class correlates with enhancer strength

Although each of the 15 enhancers tested is active broadly across the eye disc when acting on a promoter in *cis*, the enhancers vary greatly in the number of cells where transvection is observed in each disc. While several parameters may influence variation in transvection by the different enhancers, a simple possibility that may contribute to their difference is the overall strength of transcriptional activation supported by each enhancer. Specifically, those enhancers that are generally strong transcriptional activators in *cis* may have a greater chance of acting on a promoter in *trans*, whereas those enhancers that act weakly in *cis* may be much less likely to activate a promoter in *trans*. To test this possibility, we first stained imaginal discs representing a subset of strong and weak class enhancers for β-gal activity, which reflects the strength of *cis*-activation. Using identical staining conditions for discs carrying each enhancer tested, we found that enhancers of the strong class tended to produce darker β-gal staining than those of the weak class (Figure 6A; data not shown). We then used quantitative RT-PCR to assess *lacZ* transcript levels in third instar eye-antennal discs from five lines each of strong and weak class enhancers (Figure 6B). Overall, we observed a >100-fold difference in *lacZ* transcript levels between the strongest and weakest enhancers. Consistent with the β-gal activity analysis, the enhancers with the highest activation of *lacZ* in *cis* tended to be of the strong class supporting transvection, whereas those with the lowest levels of *cis*-activity tended to be of the weak transvection class. Comparison of *lacZ* transcript levels grouped by enhancer class (strong *vs.* weak) showed that this difference is significant ($P = 0.036$, Mann–Whitney *U*-test), supporting that an enhancer's strength in *cis* is a major determinant of its capacity to act in *trans*.

To further support a link between enhancer strength and transvection class, we created a construct carrying three tandem copies of the weak class enhancer *pax*. Multimerization of enhancer and/or transcription factor binding site sequences has been previously employed in transgenic organisms to boost an enhancer's strength of activation, likely by recruiting higher local concentrations of specific transcriptional activators (*e.g.*, Moses and Rubin 1991; Scott *et al.* 1999; Horn *et al.* 2000; Zimmerman *et al.* 2000). Quantitative RT-PCR showed that *lacZ* transcript levels in *paxpaxpax-LTL-lacZ* eye-antennal discs are approximately sevenfold higher than those produced by *pax-LTL-lacZ*, indicating an increased level of *cis*-activity by the multimerized enhancer (data not shown). Interestingly, staining of *paxpaxpax-LTL-lacZ* eye-antennal discs with antibodies to β-gal showed a pattern of *cis*-expression noticeably broader than that expected for cone cells, the established specificity of the *pax* enhancer (Figure S6). Higher resolution imaging confirmed that, in discs carrying *paxpaxpax-LTL-lacZ*, β-gal staining overlapped that of the neuronal marker anti-Elav (Figure 7A), demonstrating that tandem multimerization of the *pax* enhancer expands its typical cell-type specificity to include neurons in addition to cone cells. When placed in *trans*
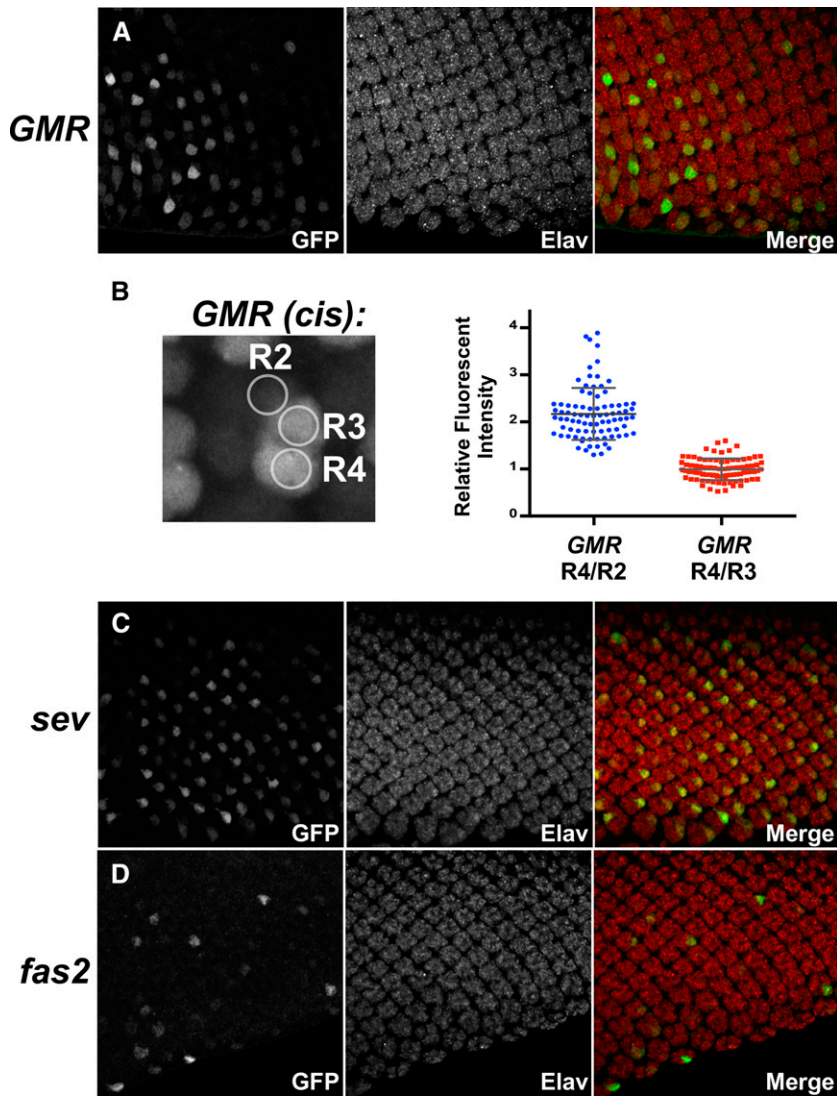
**Figure 5** Cell-type specificity of transvection correlates with strength and timing of *cis*-activity. (A) Eye discs showing *trans*-activation of *hsp70-GFP* by the enhancer *GMR*. Costaining with anti-Elav shows that the majority of GFP-positive cells are either R3 or R4. (B) Image shows a single ommatidial cluster with GFP driven in *cis* by *GMR*. The positions of R2–R4 are highlighted. Relative fluorescent intensities of R4 *vs.* R2 (blue) or R3 (red) show higher R4 expression relative to R2 (2.17 ± 0.55), but equivalent expression in R4 and R3 (1.06 ± 0.26). (C and D) Eye discs showing *trans*-activation of *hsp70-GFP* by *sev* (C) or *fas2* (D) enhancers with costaining for the neuronal marker Elav.

to *hsp70-GFP, paxpaxpax-LTL-lacZ* produced robust GFP fluorescence in many cells posterior to the morphogenetic furrow in all discs analyzed ($n = 11$), a pattern consistent with the strong class of enhancers and in stark contrast to the weak *trans*-activation of *hsp70-GFP* produced by a single copy of the *pax* enhancer (Figure 7B). Consistent with the broad cell-type specificity of the multimerized enhancer, costaining of discs carrying *paxpaxpax-LTL-lacZ* in *trans* to *hsp70-GFP* with either anti-Elav or anti-Cut showed that GFP fluorescence overlapped both neurons and cone cells (Figure 7, C and D). Thus, increasing enhancer strength via multimerization, which in this case increases transcriptional activity and expands the number of cells in which the enhancer is active, can convert an enhancer with barely detectable *trans*-activity to one with robust *trans*-activity.

### Analysis of wing enhancers further supports a link between enhancer strength and transvection

To determine whether a link between enhancer strength in *cis* and transvection may be common to enhancers of other

tissues, we created *LTL-lacZ* constructs carrying three different enhancers that are active in the third instar larval wing disc: *Ser*, *sal*, and *ct(2.7)* (Table 1). Qualitative β-gal staining shows that *Ser* is the strongest of the enhancers, producing dark staining at the wing margin, while *sal* and *ct(2.7)* act more weakly in *cis* (Figure 8A). When placed in *trans* to *hsp70-GFP*, 14/14 discs carrying the *Ser* enhancer showed robust GFP fluorescence. In contrast, *trans*-activation of *hsp70-GFP* by the *ct(2.7)* enhancer was comparatively weaker and variable, and the *sal* enhancer produced no detectable GFP in *trans*, even when the promoter in *cis* was removed via Cre/loxP-mediated recombination (Figure 8A and data not shown). Further testing of the three enhancers using *hsp70-FLP* and the G-TRACE cassette demonstrated strong transvection by *Ser* in all discs, but weak transvection by *ct(2.7)* and *sal*, with just a few GFP-positive cells in the activation domains of each enhancer (Figure 8A). An exception was the air sac primordium (ASP) in discs carrying the *ct(2.7)* enhancer, which showed strong β-gal staining and more consistent GFP fluorescence in the

**Table 2 Cell-type specificity of *hsp70-GFP trans*-activation**

| Enhancer | Ommatidial clusters scored | R3 positive (%) | R4 positive (%) | Other R cell positive (%) |
|---|---|---|---|---|
| *GMR* | 145 | 57 | 84 | 9 |
| *sev* | 203 | 27 | 84 | 3[a] |
| *fas2* | 194 | 5 | 11 | 9 |

[a] One Elav-negative cell, scored a cone cell, was also positive for GFP.



**Figure 6** Enhancer transvection class correlates with enhancer strength in *cis*. (A) β-Gal staining of eye discs from representative strong and weak class enhancers. All discs were stained under identical conditions. (B) Relative levels of *lacZ* mRNA generated by different enhancers as assessed by quantitative RT-PCR from eye-antennal discs. Levels are normalized to the enhancer ey (= 1.0). Enhancers of the strong transvection class were more likely to drive higher levels of *lacZ* mRNA in *cis*.

G-TRACE system relative to the wing margin, consistent with a link between enhancer strength and transvection.

As a final test, we multimerized three tandem copies of the weak *sal* enhancer to create *salsalsal-LTL-lacZ*. We predicted that the multimerized version would boost *cis*-activity and that it would subsequently show robust fluorescence when placed in *trans* to *hsp70-GFP*. Indeed, quantitative RT-PCR showed that *lacZ* transcript levels were >45 times higher in wing discs from flies carrying the *salsalsal* enhancer relative to those without multimerization, and β-gal activity assays showed intense staining that was restricted to the pattern expected for a single copy of the sal enhancer (Figure 8B; Figure S1). Notably, *trans*-activation of *hsp70-GFP*, which was not detectable for the single copy of *sal*, was robust and easily detected in all discs carrying *salsalsal-LTL-lacZ* (*n* = 9) (Figure 8C). Thus, enhancers of the wing disc further support a relationship between enhancer strength and transvection.

### Factors beyond enhancer strength also influence transvection

The *ct(2.7)* enhancer described above is a large 2.7-kb fragment derived from a region ∼80 kb upstream of the *ct* gene promoter (Jack *et al.* 1991). We also tested a smaller 668-bp *ct* enhancer fragment, *ct(668)*, that is contained within the larger 2.7-kb enhancer and is also capable of driving expression at the wing margin of third instar wing discs (Guss *et al.* 2001). Quantitative RT-PCR on wing disc tissue showed that *lacZ* transcript levels from the smaller fragment are roughly twofold higher than that of the larger fragment (Figure 9A), although β-gal staining suggests that both large and small *ct* enhancers are weaker than the *Ser* enhancer described above (Figure 8A and Figure 9B). Notably, although *cis*-activation by the smaller *ct(668)* enhancer appears to be stronger than that of the larger *ct(2.7)* enhancer, *trans*-activation of *hsp70-GFP* by the small enhancer was not observed (0/8 discs; Figure 9C) as it was for the large enhancer (10/10 discs; Figure 8A). Analysis of the smaller *ct(668)* enhancer using the G-TRACE system was complicated by the widespread appearance of large patches of GFP-positive cells, presumably due to nonspecific *trans*-activation of the *hsp70-FLP* transgene in precursor cells, although GFP-positive cells could also be seen at the wing margin in some discs (Figure S7). In sum, although there is an overall correlation between the strength of an enhancer acting in *cis* and its capacity to support transvection, additional factors likely also contribute to the ability of some enhancers to act in *trans*.
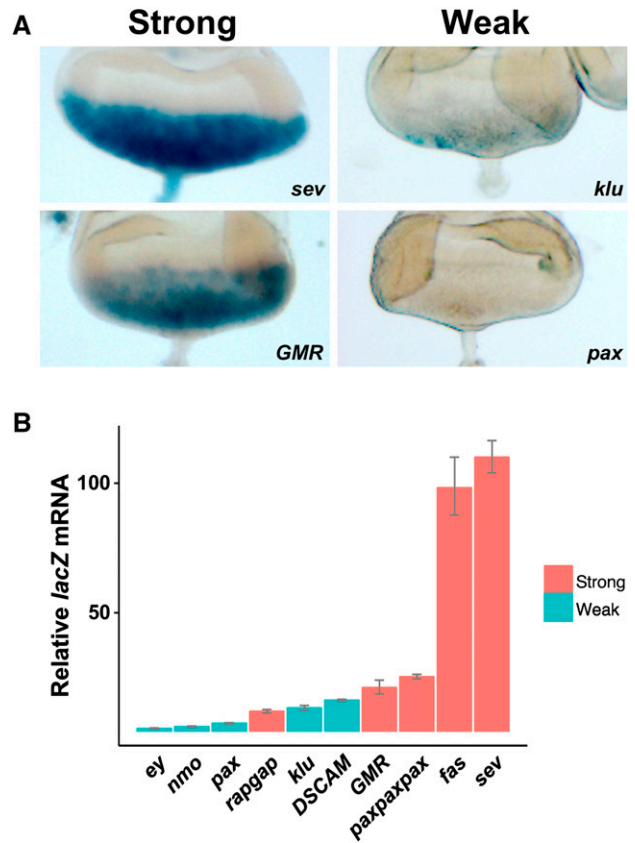
### Discussion

The generality of gene regulation via transvection in *Drosophila* has been a long-standing question. Prior classical data provided evidence for enhancer action in *trans* at a handful of loci, demonstrating that several *Drosophila* enhancers can activate a promoter on a separate chromosome. However, in the majority of these cases, transvection was uncovered serendipitously through the chance isolation of specific types of mutations, and it remained unclear whether enhancers that can act in *trans* represent a distinct class of regulatory elements. In this study, we systematically analyzed known enhancers for a capacity to act in *trans*. We focused our analysis on tissues known to support transvection and created a system based on a weak promoter in *cis* to each enhancer to optimize the likelihood of observing enhancer action in *trans*. Our data showed evidence of transvection for all enhancers tested, albeit at greatly varying levels. In sum, our data support the hypothesis that enhancers that act in *trans* do not represent a special functional class; rather, it is plausible that any enhancer has the capacity to act on a promoter of a closely paired chromosome.
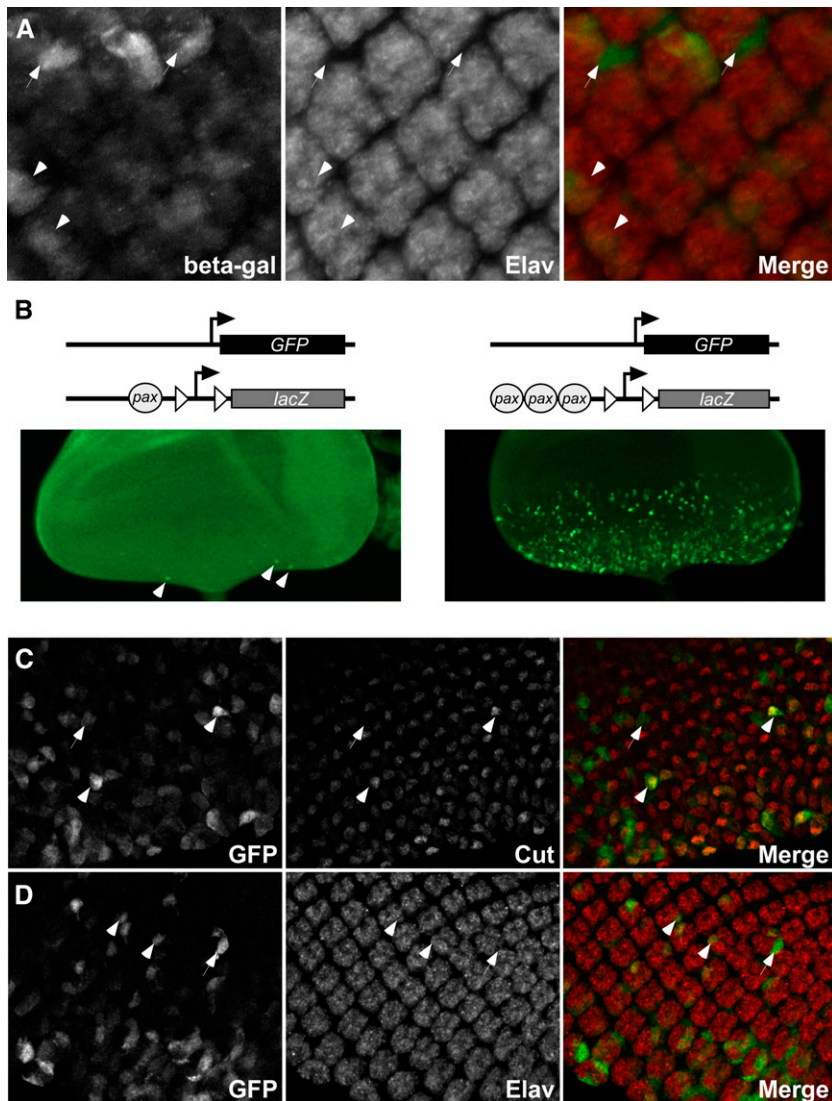
**Figure 7** Multimerization of the *pax* enhancer increases its capacity to support transvection. (A) Staining of eye discs carrying *paxpaxpax-LTL-lacZ* with antibodies against β-gal and Elav. Arrowheads show β-gal-positive cells that overlap Elav-positive neurons, whereas arrows show cells with positions consistent with cone cells. Note that the signal for β-gal appears weak at high resolution due to the weak nature of the LTL promoter. (B) Representative eye discs carrying *pax* or *paxpaxpax* showing *trans*-activation of *hsp70-GFP*. Multimerization of the *pax* enhancer results in a change from weak to strong transvection class. (C and D) Eye discs showing *paxpaxpax* activation of *hsp70-GFP* in *trans*, with staining for GFP and either the cone cell marker Cut (C) or the neuronal marker Elav (D). Cells showing overlap (arrowheads) and no overlap (arrows) of signals are visible for both markers.

A previous study by Mellert and Truman (2012) used a related transgenic approach to test 21 neural-specific enhancers for an ability to support transvection and found no evidence for enhancer action in *trans* for roughly half of their sample, contrasting the results of our study. The two studies differ in several fundamental respects; perhaps most importantly, we used a weak (or absent) promoter in *cis* and a strong promoter in *trans*, whereas the prior test of 21 neural enhancers relied on transgenes carrying identical strong promoters in *cis* and in *trans*. Thus, it is conceivable that enhancers that were scored negatively for transvection in the previous study were, in fact, restricted from acting in *trans* at detectable levels due to competition from the promoter in *cis*, whereas other enhancers in the study may have been less sensitive to the promoter in *cis*. Consistent with this hypothesis, the enhancers of the *yellow* gene do not appear to act in *trans* in the presence of a strong promoter in *cis* (Geyer *et al.* 1990; Morris *et al.* 1999), whereas enhancers from other genes will show low levels of transvection when juxtaposed to a strong *cis*-promoter and higher levels of transvection in the

absence of a *cis*-promoter (Martinez-Laborda *et al.* 1992; Casares *et al.* 1997; Gohl *et al.* 2008; Bateman *et al.* 2012a; Mellert and Truman 2012). We also found that two enhancers from our study differed in sensitivity to a promoter in *cis*, as Cre/loxP removal of the *LTL* promoter increased transvection by the *klu* enhancer but not by the *pax* enhancer. In sum, the differences between the present study and that of Mellert and Truman (2012) likely reflect the use of different strategies, with one study focusing on conditions favorable for observing transvection and the other representing a more stringent test.

### Enhancer strength is a major determinant of transvection

Our data indicate that the varying levels of transvection displayed by different enhancers are largely due to their differing strengths, as broadly defined by the activation of a promoter in *cis*. This conclusion was supported in part by quantitative RT-PCR data from diverse enhancers that act in the eye disc and by multimerization of two weak class enhancers that led to increased *cis*-activity and nonadditive
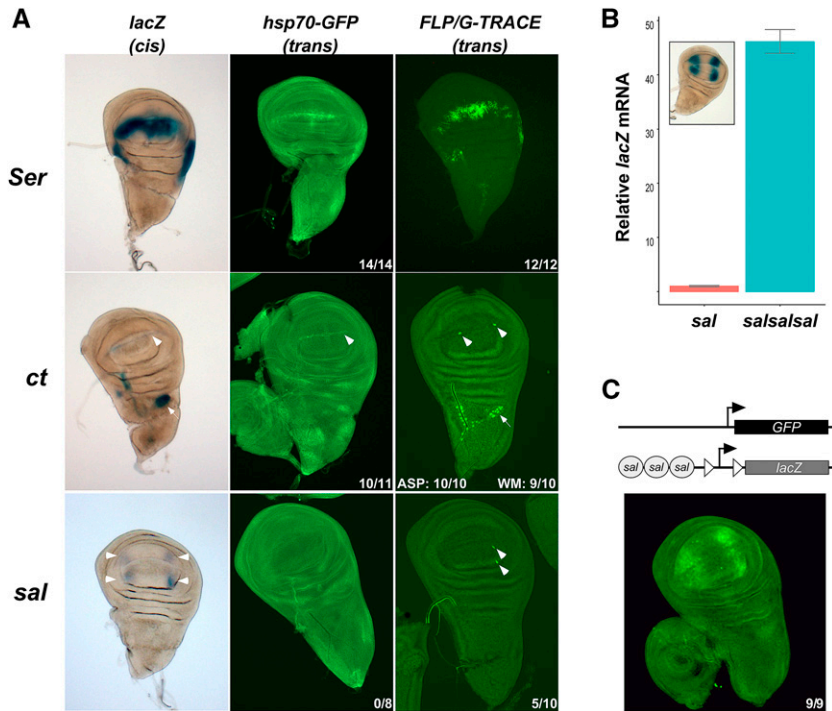
**Figure 8** Analysis of wing enhancers further supports a link between enhancer strength and transvection class. (A) β-Gal staining and *trans*-activation of *hsp70-GFP* and the *hsp70-FLP*/G-TRACE system is shown for the wing disc enhancers *Ser*, *ct(2.7)*, and *sal*. *Ser*, the strongest enhancer in *cis*, shows more consistent and robust *trans*-action than the weaker *ct* and *sal* enhancers. Arrowheads highlight β-gal-positive or GFP-positive cells in the expected domains of the wing pouch for *ct* and *sal*; arrows marks the air sac primordium (ASP). The fraction of scored discs that showed GFP-positive cells is given for each test for *trans*-activation. The ASP was not scored in discs activating *hsp70-GFP* due to high levels of background fluorescence in that region. (B) Multimerization of *sal* to create *salsalsal* increases *cis*-expression ~45-fold as assessed by quantitative RT-PCR on wing discs. Data represent two independent experiments. Inset shows β-gal staining of a wing disc carrying *salsalsal-LTL-lacZ*. (C) *salsalsal* activates *hsp70-GFP* in *trans* at high levels relative to a single copy of the *sal* enhancer.

conversion to strong class transvection phenotypes. Formally, an enhancer's output in *cis* could impact transvection in at least two nonmutually exclusive ways; in one model, the transcriptional output of an enhancer in an individual cell would influence whether or not transvection could occur in that cell, or, in another model, the proportion of cells of a given tissue in which the enhancer is active could create more or fewer opportunities for transvection to occur in that tissue. Our data are consistent with both of these models for the influence of enhancer strength on transvection. Specifically, multimerization of the *sal* enhancer dramatically increases transcriptional output in *cis*, but does not perceptibly alter the spatial pattern of the enhancer's activity, implying that the impact of multimerization on transvection reflects increased transcription on a per-cell basis. Our data regarding the strong bias for *sev* and *GMR* transvection for R3 and R4, where activity in *cis* is strongest in early developing ommatidia, are also consistent with this model. In contrast, multimerization of the *pax* enhancer appears to increase both the transcriptional output of individual cells and the range of cell types in which the enhancer is active. Note that prior analysis of this enhancer also demonstrated a change in cell-type specificity to include neurons when the sequence was rearranged rather than multimerized (Swanson *et al.* 2010), and, more generally, strengthening the efficiency of reporter construct output has previously been shown to expand the detectable cell types in which an enhancer is active (Pfeiffer *et al.* 2010). In the case of the multimerized *pax* enhancer, it is likely that its increased ability to act in *trans* relative to a single *pax* enhancer reflects both higher rates of transcription per cell and increased opportunites for transvection via activity in an expanded number of cells.

In sum, our data support a model wherein, when acting in *cis*, an enhancer of the weak transvection class activates fewer rounds of transcription relative to a strong class enhancer, either due to lower levels of transcription in each cell, fewer cells in which the enhancer is active, or both. When acting in *trans*, a weak class enhancer is less likely to activate detectable levels of transcription in any given cell within the tissue, leading to fewer GFP-positive cells relative to a strong enhancer.

### Factors other than enhancer strength influence transvection

Despite a general relationship between enhancer strength and *trans*-action, exceptions within our data indicate that other factors likely play a role in transvection for some enhancers and further highlight potential differences between *cis*- and *trans*-activity. For example, although the bias for transvection by *GMR* and *sev* in photoreceptors R3 and R4 may be explained in part by the strength of the enhancers' *cis*-activity in those cells, we also found that transvection was observed more frequently in R4 than in any other cell, including R3. However, in the case of the *GMR* enhancer, we found no significant different between *cis*-activity in R3 and R4 as assessed by levels of GFP fluorescence. Thus, it is possible that factors and/or parameters that influence transvection may exist at different levels in different cell types and at different times of development. This possibility is consistent with prior observations; for example, analysis of transvection in the larval nervous system implied that certain neural cell types were more conducive to transvection than others (Mellert and Truman 2012). Furthermore, factors that promote or hinder somatic homolog pairing, a requirement for
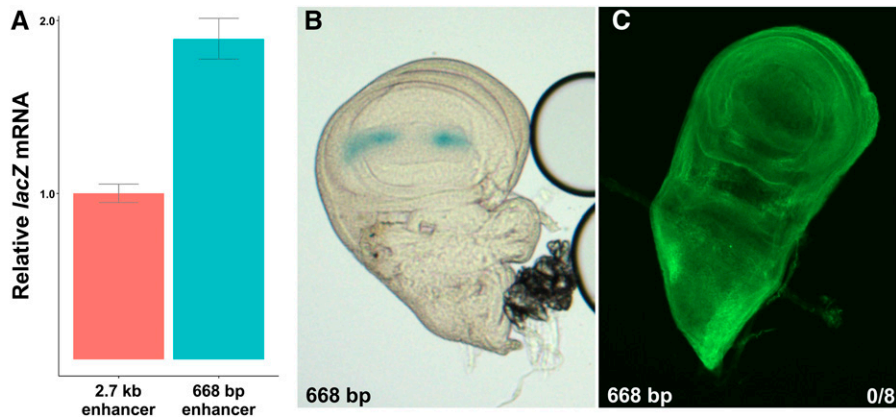
**Figure 9** Factors beyond enhancer strength may also contribute to transvection. (A) Truncated fragment of the 2.7-kb *ct* enhancer produces higher levels of *lacZ* expression in *cis* as assessed by quantitative RT-PCR. Data represent three independent experiments. (B) β-Gal staining shows the *ct(668)* enhancer fragment is active at the wing margin. (C) No *trans*-activation of *hsp70-GFP* is detected at the wing margin for the shorter *ct* enhancer fragment.

transvection, have been identified, and may function differently in different cell types (Hartl *et al.* 2008; Bateman *et al.* 2012b; Joyce *et al.* 2012). Finally, data based on DNA-FISH show high levels of somatic homolog pairing in third instar larvae, but lower levels during embryogenesis, which would likely negatively impact transvection in early tissues (Fung *et al.* 1998). Consistent with this, very few examples of transvection have been described in *Drosophila* embryos (Hendrickson and Sakonju 1995; Ronshaugen and Levine 2004; Fujioka *et al.* 2016) relative to later developmental time points. A broad study of enhancer action in *trans* across different tissues and developmental time points would be highly informative of different parameters that affect transvection.

In addition to biases in cell-type specificity of transvection, our data support the existence of DNA sequences that can modulate transvection. In the case of the *ct* enhancer, a large fragment with moderate expression at the wing margin showed a greater degree of transvection than did a smaller enhancer fragment with more robust expression at the wing margin. It is possible that the differences in *trans*-activity observed for these enhancer fragments are simply caused by their different sizes; for example, a larger fragment may alter local pairing between the two homologous chromosomes in a manner that facilitates access to the promoter in *trans*. However, the other enhancers in our study show no correlation between fragment size and strength of transvection (Table 1; data not shown), indicating that a size effect is not a general phenomenon. An intriguing possibility is that the larger *ct* enhancer fragment could possess sequences that aid in targeting distal promoters, including promoters in *trans*, that are not present in the smaller fragment. Indeed, the *ct* enhancer is normally 80 kb away from its promoter target, and sequences that promote long-range enhancer–promoter interactions in *cis* and in *trans* have been characterized for other genes (Hopmann *et al.* 1995; Zhou and Levine 1999; Calhoun *et al.* 2002; Calhoun and Levine 2003; Lin 2003; Akbari *et al.* 2008; Fujioka *et al.* 2009; Majumder *et al.* 2015). The notion that variation in transvection could be partially dependent on factors beyond enhancer strength is supported by previous studies. For

example, pairing the same enhancer fragment with transgenes carrying different genomic fragments upstream of a *trans*-promoter can result in varying levels of transvection, suggesting that "compatibility" of paired sequences is important for robust enhancer action in *trans* (Mellert and Truman 2012). Furthermore, insulator sequences have previously been shown to have a positive influence on transvection and other long-distance enhancer–promoter interactions (Kravchenko *et al.* 2005; Schoborg *et al.* 2013; Fujioka *et al.* 2016). In addition, some examples of transvection at the abdominal-B locus require a 10-kb sequence in addition to the enhancer (Hopmann *et al.* 1995), and transvection of the *Men* locus varies greatly across genetic backgrounds (Lum and Merritt 2011). Thus, while our data support that an enhancer's strength in *cis* is also reflected in its action in *trans*, it is likely that other sequences can further modulate transvection.

Finally, we cannot exclude the possibility that some enhancers act with different specificity in *trans* relative to their activities in *cis*. We were unable to reliably determine the cell-type specificity of transvection by many weak class enhancers due to the weak GFP staining produced by *trans*-activation of *hsp70-GFP* and complications of spontaneous FLP activity using the G-TRACE system. However, we were surprised to find that the *Rh4* enhancer supported weak class transvection in the larval eye disc, given that the *Rh4* gene is normally activated in this tissue at a later period in development (Pollock and Benzer 1988; Fortini and Rubin 1990). It is possible that the enhancer fragment used in our analysis also shows activity in the larval eye disc in *cis* that is not representative of the wild-type expression pattern, although we were unable to confirm this using β-gal staining and the weak LTL promoter (data not shown). Alternatively, it may be that low-level activation of a promoter in *trans* can occur outside the normal spatiotemporal domain of a given enhancer's *cis*-expression. Consistent with this, prior analysis has shown that altering the identity of the promoter downstream of an enhancer in *cis* can also alter its cell-type specificity (Mellert and Truman 2012), implying an inherent fluidity of enhancer function in different cell identities that depends on the nature of enhancer–promoter communication.

### Does transvection play a role in the wild?

Studies of transvection in *Drosophila* have traditionally relied on mutant and/or transgenic organisms where evidence of gene regulation in *trans* can be easily observed. While these analyses have provided great insight into mechanisms of enhancer action in *trans*, they leave outstanding questions of a potential role for transvection in wild-type organisms. Does somatic homolog pairing and/or transvection provide direct benefit to *Drosophila* and/or other organisms? Recent analysis has shown that programmed stochastic expression of Rh3 and Rh4 opsins in *Drosophila* is controlled in part by *trans*-interactions between homologs of the *Spineless* gene (Johnston and Desplan 2014), and other interallelic interactions that help to pattern gene expression may also exist. Furthermore, for the promoters of some genes, it may be that the combined input of enhancers in *cis* and *trans* can aid in ensuring tight regulation of patterned gene expression, as has been postulated for seemingly redundant enhancers found at some developmental genes (so-called "shadow" enhancers) (reviewed by Lagha *et al.* 2012). Given the wide range of transvection strength observed in our study, our data suggest that such combined action of enhancers in *cis* and *trans* may be more relevant to some genes than others. Consistent with this, enhancer action in *trans* observed using classical alleles of different genes can produce widely varying levels of transcription, from ~1% or less of wild-type levels using certain alleles of *yellow* (Morris *et al.* 2004), to near 100% of wild-type activity for some alleles of the *Men* and *sn-Glycerol-3-Phosphate Dehydrogenase* genes (Gibson *et al.* 1999; Lum and Merritt 2011). In addition, many other types of regulatory sequences, including insulators and Polycomb response elements, may function more efficiently when paired or clustered (reviewed by Bantignies and Cavalli 2011; Herold *et al.* 2012). In non-Dipteran organisms, where somatic homolog pairing is the exception rather than the rule, interchromosomal interactions between nonhomologous sequences are routinely uncovered in whole-genome interaction assays (Lieberman-Aiden *et al.* 2009; Duan *et al.* 2010; Sexton *et al.* 2012; van de Werken *et al.* 2012; Nagano *et al.* 2013; Zhang *et al.* 2013), and specific *trans*-interactions have been linked to several examples of gene regulation (Spilianakis *et al.* 2005; Bacher *et al.* 2006; Xu *et al.* 2006; Apostolou and Thanos 2008; Sandhu *et al.* 2009; Markenscoff-Papadimitriou *et al.* 2014; Patel *et al.* 2014). Thus, it appears that interchromosomal communication is adaptable to the different global principles for genome organization present in Dipteran and non-Dipteran organisms and likely plays a role in maintaining correct patterns of gene expression across diverse species.

### Acknowledgments

### Literature Cited

Aerts, S., X. J. Quan, A. Claeys, M. Naval Sanchez, P. Tate *et al.*, 2010  Robust target gene discovery through transcriptome perturbations and genome-wide enhancer predictions in Drosophila uncovers a regulatory basis for sensory specification. PLoS Biol. 8: e1000435.

Akbari, O. S., E. Bae, H. Johnsen, A. Villaluz, D. Wong *et al.*, 2008  A novel promoter-tethering element regulates enhancer-driven gene expression at the bithorax complex in the Drosophila embryo. Development 135: 123–131.

Apostolou, E., and D. Thanos, 2008  Virus infection induces NF-kappaB-dependent interchromosomal associations mediating monoallelic IFN-beta gene expression. Cell 134: 85–96.

Bacher, C. P., M. Guggiari, B. Brors, S. Augui, P. Clerc *et al.*, 2006  Transient colocalization of X-inactivation centres accompanies the initiation of X inactivation. Nat. Cell Biol. 8: 293–299.

Bantignies, F., and G. Cavalli, 2011  Polycomb group proteins: repression in 3D. Trends Genet. 27: 454–464.

Bateman, J. R., and C. T. Wu, 2008  A simple polymerase chain reaction-based method for the construction of recombinase-mediated cassette exchange donor vectors. Genetics 180: 1763–1766.

Bateman, J. R., A. M. Lee, and C. T. Wu, 2006  Site-specific transformation of Drosophila via phiC31 integrase-mediated cassette exchange. Genetics 173: 769–777.

Bateman, J. R., J. E. Johnson, and M. N. Locke, 2012a  Comparing enhancer action in *cis* and in *trans*. Genetics 191: 1143–1155.

Bateman, J. R., E. Larschan, R. D'Souza, L. S. Marshall, K. E. Dempsey *et al.*, 2012b  A genome-wide screen identifies genes that affect somatic homolog pairing in Drosophila. G3 (Bethesda) 2: 731–740.

Bing, X., T. Z. Rzeznicak, J. R. Bateman, and T. J. Merritt, 2014  Transvection-based gene regulation in Drosophila is a complex and plastic trait. G3 (Bethesda) 4: 2175–2187.

Blochlinger, K., L. Y. Jan, and Y. N. Jan, 1993  Postembryonic patterns of expression of cut, a locus regulating sensory organ identity in Drosophila. Development 117: 441–450.

Bosco, G., 2012  Chromosome pairing: a hidden treasure no more. PLoS Genet. 8: e1002737.

Bowtell, D. D., B. E. Kimmel, M. A. Simon, and G. M. Rubin, 1989  Regulation of the complex pattern of sevenless expression in the developing Drosophila eye. Proc. Natl. Acad. Sci. USA 86: 6245–6249.

Bowtell, D. D., T. Lila, W. M. Michael, D. Hackett, and G. M. Rubin, 1991  Analysis of the enhancer element that controls expression of sevenless in the developing Drosophila eye. Proc. Natl. Acad. Sci. USA 88: 6853–6857.

Calhoun, V. C., and M. Levine, 2003  Long-range enhancer-promoter interactions in the Scr-Antp interval of the Drosophila Antennapedia complex. Proc. Natl. Acad. Sci. USA 100: 9878–9883.

Calhoun, V. C., A. Stathopoulos, and M. Levine, 2002  Promoter-proximal tethering elements regulate enhancer-promoter specificity in the Drosophila Antennapedia complex. Proc. Natl. Acad. Sci. USA 99: 9243–9247.

Casares, F., W. Bender, J. Merriam, and E. Sanchez-Herrero, 1997   Interactions of Drosophila Ultrabithorax regulatory regions with native and foreign promoters. Genetics 145: 123–137.

Chen, J. L., K. L. Huisinga, M. M. Viering, S. A. Ou, C. T. Wu *et al.*, 2002   Enhancer action in trans is permitted throughout the Drosophila genome. Proc. Natl. Acad. Sci. USA 99: 3723–3728.

Cooper, M. T., and S. J. Bray, 1999   Frizzled regulation of Notch signalling polarizes cell fate in the Drosophila eye. Nature 397: 526–530.

Coulthard, A. B., N. Nolan, J. B. Bell, and A. J. Hilliker, 2005   Transvection at the vestigial locus of Drosophila melanogaster. Genetics 170: 1711–1721.

Domingos, P. M., M. Mlodzik, C. S. Mendes, S. Brown, H. Steller *et al.*, 2004   Spalt transcription factors are required for R3/R4 specification and establishment of planar cell polarity in the Drosophila eye. Development 131: 5695–5702.

Duan, Z., M. Andronescu, K. Schutz, S. McIlwain, Y. J. Kim *et al.*, 2010   A three-dimensional model of the yeast genome. Nature 465: 363–367.

Evans, C. J., J. M. Olson, K. T. Ngo, E. Kim, N. E. Lee *et al.*, 2009   G-TRACE: rapid Gal4-based cell lineage analysis in Drosophila. Nat. Methods 6: 603–605.

Flores, G. V., H. Duan, H. Yan, R. Nagaraj, W. Fu *et al.*, 2000   Combinatorial signaling in the specification of unique cell fates. Cell 103: 75–85.

Fortini, M. E., and G. M. Rubin, 1990   Analysis of cis-acting requirements of the Rh3 and Rh4 genes reveals a bipartite organization to rhodopsin promoters in Drosophila melanogaster. Genes Dev. 4: 444–463.

Fujioka, M., X. Wu, and J. B. Jaynes, 2009   A chromatin insulator mediates transgene homing and very long-range enhancer-promoter communication. Development 136: 3077–3087.

Fujioka, M., H. Mistry, P. Schedl, and J. B. Jaynes, 2016   Determinants of chromosome architecture: insulator pairing in cis and in trans. PLoS Genet. 12: e1005889.

Fung, J. C., W. F. Marshall, A. F. Dernburg, D. A. Agard, and J. W. Sedat, 1998   Homologous chromosome pairing in Drosophila melanogaster proceeds through multiple independent initiations. J. Cell Biol. 141: 5–20.

Gallo, S. M., D. T. Gerrard, D. Miner, M. Simich, B. Des Soye *et al.*, 2011   REDfly v3.0: toward a comprehensive database of transcriptional regulatory elements in Drosophila. Nucleic Acids Res. 39: D118–D123.

Gelbart, W. M., 1982   Synapsis-dependent allelic complementation at the decapentaplegic gene complex in Drosophila melanogaster. Proc. Natl. Acad. Sci. USA 79: 2636–2640.

Geyer, P. K., M. M. Green, and V. G. Corces, 1990   Tissue-specific transcriptional enhancers may act in trans on the gene located in the homologous chromosome: the molecular basis of transvection in Drosophila. EMBO J. 9: 2247–2256.

Gibson, J. B., D. S. Reed, S. Bartoszewski, and A. V. Wilks, 1999   Structural changes in the promoter region mediate transvection at the sn-glycerol-3-phosphate dehydrogenase gene of Drosophila melanogaster. Biochem. Genet. 37: 301–315 (corrigendum: Biochem. Genet. 2000 38: 201–202).

Gohl, D., M. Muller, V. Pirrotta, M. Affolter, and P. Schedl, 2008   Enhancer blocking and transvection at the Drosophila apterous locus. Genetics 178: 127–143.

Guss, K. A., C. E. Nelson, A. Hudson, M. E. Kraus, and S. B. Carroll, 2001   Control of a genetic regulatory network by a selector gene. Science 292: 1164–1167.

Halder, G., P. Callaerts, S. Flister, U. Walldorf, U. Kloter *et al.*, 1998   Eyeless initiates the expression of both sine oculis and eyes absent during Drosophila compound eye development. Development 125: 2181–2191.

Hartl, T. A., H. F. Smith, and G. Bosco, 2008   Chromosome alignment and transvection are antagonized by condensin II. Science 322: 1384–1387.

Hauck, B., W. J. Gehring, and U. Walldorf, 1999   Functional analysis of an eye specific enhancer of the eyeless gene in Drosophila. Proc. Natl. Acad. Sci. USA 96: 564–569.

Hendrickson, J. E., and S. Sakonju, 1995   Cis and trans interactions between the iab regulatory regions and abdominal-A and abdominal-B in Drosophila melanogaster. Genetics 139: 835–848.

Herold, M., M. Bartkuhn, and R. Renkawitz, 2012   CTCF: insights into insulator function during development. Development 139: 1045–1057.

Hopmann, R., D. Duncan, and I. Duncan, 1995   Transvection in the iab-5,6,7 region of the bithorax complex of Drosophila: homology independent interactions in trans. Genetics 139: 815–833.

Horn, C., B. Jaunich, and E. A. Wimmer, 2000   Highly sensitive, fluorescent transformation marker for Drosophila transgenesis. Dev. Genes Evol. 210: 623–629.

Jack, J., D. Dorsett, Y. Delotto, and S. Liu, 1991   Expression of the cut locus in the Drosophila wing margin is required for cell type specification and is regulated by a distant enhancer. Development 113: 735–747.

Johnston, Jr., R. J., and C. Desplan, 2014   Interchromosomal communication coordinates intrinsically stochastic expression between alleles. Science 343: 661–665.

Joyce, E., B. Williams, T. Xie, and C.-t. Wu, 2012   Identification of genes that promote or antagonize somatic homolog pairing using a high-throughput FISH-based screen. PLoS Genet. 8: e1002667.

Juni, N., and D. Yamamoto, 2009   Genetic analysis of chaste, a new mutation of Drosophila melanogaster characterized by extremely low female sexual receptivity. J. Neurogenet. 23: 329–340.

Kassis, J. A., E. P. VanSickle, and S. M. Sensabaugh, 1991   A fragment of engrailed regulatory DNA can mediate transvection of the white gene in Drosophila. Genetics 128: 751–761.

Kravchenko, E., E. Savitskaya, O. Kravchuk, A. Parshikov, P. Georgiev *et al.*, 2005   Pairing between gypsy insulators facilitates the enhancer action in trans throughout the Drosophila genome. Mol. Cell. Biol. 25: 9283–9291.

Lagha, M., J. P. Bothma, and M. Levine, 2012   Mechanisms of transcriptional precision in animal development. Trends Genet. 28: 409–416.

Leiserson, W. M., N. M. Bonini, and S. Benzer, 1994   Transvection at the eyes absent gene of Drosophila. Genetics 138: 1171–1179.

Lewis, E. B., 1954   The theory and application of a new method of detecting chromosomal rearrangements in Drosophila melanogaster. Am. Nat. 88: 225.

Lieberman-Aiden, E., N. L. van Berkum, L. Williams, M. Imakaev, T. Ragoczy *et al.*, 2009   Comprehensive mapping of long-range interactions reveals folding principles of the human genome. Science 326: 289–293.

Lin, Q., 2003   The promoter targeting sequence facilitates and restricts a distant enhancer to a single promoter in the Drosophila embryo. Development 130: 519–526.

Lum, T. E., and T. J. Merritt, 2011   Nonclassical regulation of transcription: interchromosomal interactions at the malic enzyme locus of Drosophila melanogaster. Genetics 189: 837–849.

Majumder, K., O. I. Koues, E. A. Chan, K. E. Kyle, J. E. Horowitz *et al.*, 2015   Lineage-specific compaction of Tcrb requires a chromatin barrier to protect the function of a long-range tethering element. J. Exp. Med. 212: 107–120.

Marin, M. C., J. R. Rodriguez, and A. Ferrus, 2004   Transcription of Drosophila troponin I gene is regulated by two conserved,

functionally identical, synergistic elements. Mol. Biol. Cell 15: 1185–1196.

Markenscoff-Papadimitriou, E., W. E. Allen, B. M. Colquitt, T. Goh, K. K. Murphy et al., 2014   Enhancer interaction networks as a means for singular olfactory receptor expression. Cell 159: 543–557.

Martinez-Laborda, A., A. Gonzalez-Reyes, and G. Morata, 1992   Trans regulation in the Ultrabithorax gene of Drosophila: alterations in the promoter enhance transvection. EMBO J. 11: 3645–3652.

Mavromatakis, Y. E., and A. Tomlinson, 2013   Switching cell fates in the developing Drosophila eye. Development 140: 4353–4361.

McKee, B. D., 2004   Homologous pairing and chromosome dynamics in meiosis and mitosis. Biochim. Biophys. Acta 1677: 165–180.

Mellert, D. J., and J. W. Truman, 2012   Transvection is common throughout the Drosophila genome. Genetics 191: 1129–1141.

Morris, J. R., J. L. Chen, P. K. Geyer, and C. T. Wu, 1998   Two modes of transvection: enhancer action in trans and bypass of a chromatin insulator in cis. Proc. Natl. Acad. Sci. USA 95: 10740–10745.

Morris, J. R., P. K. Geyer, and C. T. Wu, 1999   Core promoter elements can regulate transcription on a separate chromosome in trans. Genes Dev. 13: 253–258.

Morris, J. R., D. A. Petrov, A. M. Lee, and C. T. Wu, 2004   Enhancer choice in cis and in trans in Drosophila melanogaster: role of the promoter. Genetics 167: 1739–1747.

Moses, K., and G. M. Rubin, 1991   Glass encodes a site-specific DNA-binding protein that is regulated in response to positional signals in the developing Drosophila eye. Genes Dev. 5: 583–593.

Nagano, T., Y. Lubling, T. J. Stevens, S. Schoenfelder, E. Yaffe et al., 2013   Single-cell Hi-C reveals cell-to-cell variability in chromosome structure. Nature 502: 59–64.

Patel, B., Y. Kang, K. Cui, M. Litt, M. S. Riberio et al., 2014   Aberrant TAL1 activation is mediated by an interchromosomal interaction in human T-cell acute lymphoblastic leukemia. Leukemia 28: 349–361.

Pfeiffer, B. D., T. T. Ngo, K. L. Hibbard, C. Murphy, A. Jenett et al., 2010   Refinement of tools for targeted gene expression in Drosophila. Genetics 186: 735–755.

Pollock, J. A., and S. Benzer, 1988   Transcript localization of four opsin genes in the three visual organs of Drosophila; RH2 is ocellus specific. Nature 333: 779–782.

Ronshaugen, M., and M. Levine, 2004   Visualization of trans-homolog enhancer-promoter interactions at the Abd-B Hox locus in the Drosophila embryo. Dev. Cell 7: 925–932.

Sandhu, K. S., C. Shi, M. Sjolinder, Z. Zhao, A. Gondor et al., 2009   Nonallelic transvection of multiple imprinted loci is organized by the H19 imprinting control region during germline development. Genes Dev. 23: 2598–2603.

Sanyal, A., B. R. Lajoie, G. Jain, and J. Dekker, 2012   The long-range interaction landscape of gene promoters. Nature 489: 109–113.

Schoborg, T., S. Kuruganti, R. Rickels, and M. Labrador, 2013   The Drosophila gypsy insulator supports transvection in the presence of the vestigial enhancer. PLoS One 8: e81331.

Scott, K. C., A. D. Taubman, and P. K. Geyer, 1999   Enhancer blocking by the Drosophila gypsy insulator depends upon insulator anatomy and enhancer strength. Genetics 153: 787–798.

Sexton, T., E. Yaffe, E. Kenigsberg, F. Bantignies, B. Leblanc et al., 2012   Three-dimensional folding and functional organization principles of the Drosophila genome. Cell 148: 458–472.

Siegal, M. L., and D. L. Hartl, 1996   Transgene coplacement and high efficiency site-specific recombination with the Cre/loxP system in Drosophila. Genetics 144: 715–726.

Southworth, J. W., and J. A. Kennison, 2002   Transvection and silencing of the Scr homeotic gene of Drosophila melanogaster. Genetics 161: 733–746.

Spilianakis, C. G., M. D. Lalioti, T. Town, G. R. Lee, and R. A. Flavell, 2005   Interchromosomal associations between alternatively expressed loci. Nature 435: 637–645.

Swanson, C. I., N. C. Evans, and S. Barolo, 2010   Structural rules and complex regulatory circuitry constrain expression of a Notch- and EGFR-regulated eye enhancer. Dev. Cell 18: 359–370.

Tomlinson, A., D. D. Bowtell, E. Hafen, and G. M. Rubin, 1987   Localization of the sevenless protein, a putative receptor for positional information, in the eye imaginal disc of Drosophila. Cell 51: 143–150.

Untergasser, A., I. Cutcutache, T. Koressaar, J. Ye, B. C. Faircloth et al., 2012   Primer3: new capabilities and interfaces. Nucleic Acids Res. 40: e115.

van de Werken, H. J., G. Landan, S. J. Holwerda, M. Hoichman, P. Klous et al., 2012   Robust 4C-seq data analysis to screen for regulatory DNA interactions. Nat. Methods 9: 969–972.

Wildonger, J., A. Sosinsky, B. Honig, and R. S. Mann, 2005   Lozenge directly activates argos and klumpfuss to regulate programmed cell death. Genes Dev. 19: 1034–1039.

Wu, C. T., and M. Howe, 1995   A genetic analysis of the Suppressor 2 of zeste complex of Drosophila melanogaster. Genetics 140: 139–181.

Xu, C., R. C. Kauffmann, J. Zhang, S. Kladny, and R. W. Carthew, 2000   Overlapping activators and repressors delimit transcriptional response to receptor tyrosine kinase signals in the Drosophila eye. Cell 103: 87–97.

Xu, N., C. L. Tsai, and J. T. Lee, 2006   Transient homologous chromosome pairing marks the onset of X inactivation. Science 311: 1149–1152.

Yan, S. J., Y. Gu, W. X. Li, and R. J. Fleming, 2004   Multiple signaling pathways and a selector protein sequentially regulate Drosophila wing development. Development 131: 285–298.

Zhang, Y., C. H. Wong, R. Y. Birnbaum, G. Li, R. Favaro et al., 2013   Chromatin connectivity maps reveal dynamic promoter-enhancer long-range associations. Nature 504: 306–310.

Zhou, J., and M. Levine, 1999   A novel cis-regulatory element, the PTS, mediates an anti-insulator activity in the Drosophila embryo. Cell 99: 567–575.

Zimmerman, J. E., Q. T. Bui, H. Liu, and N. M. Bonini, 2000   Molecular genetic analysis of Drosophila eyes absent mutants reveals an eye enhancer element. Genetics 154: 237–246.

*Communicating editor: P. K. Geyer*

# GENETICS

## The Capacity to Act in *Trans* Varies Among *Drosophila* Enhancers

Amanda J. Blick, Ilana Mayer-Hirshfeld, Beatriz R. Malibiran, Matthew A. Cooper, Pieter A. Martino,
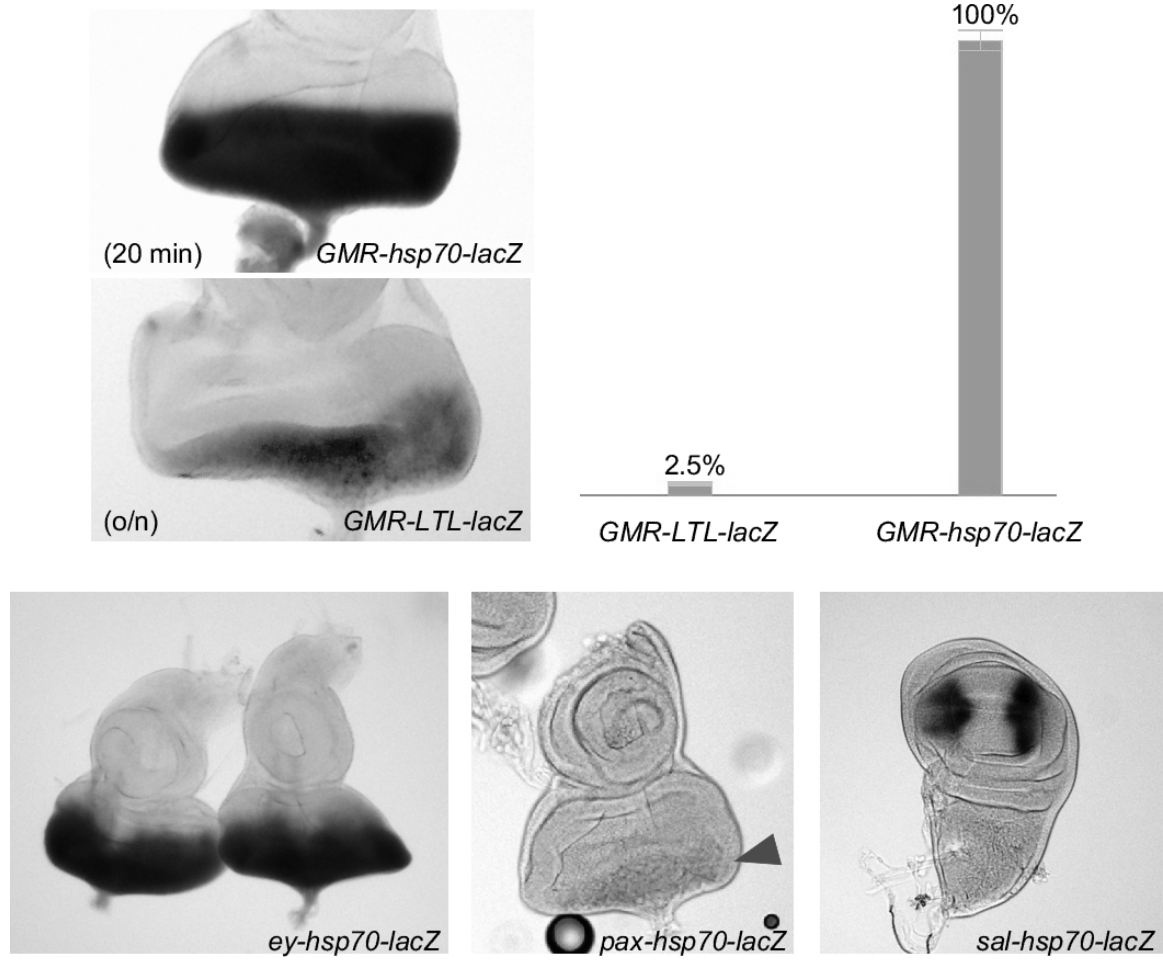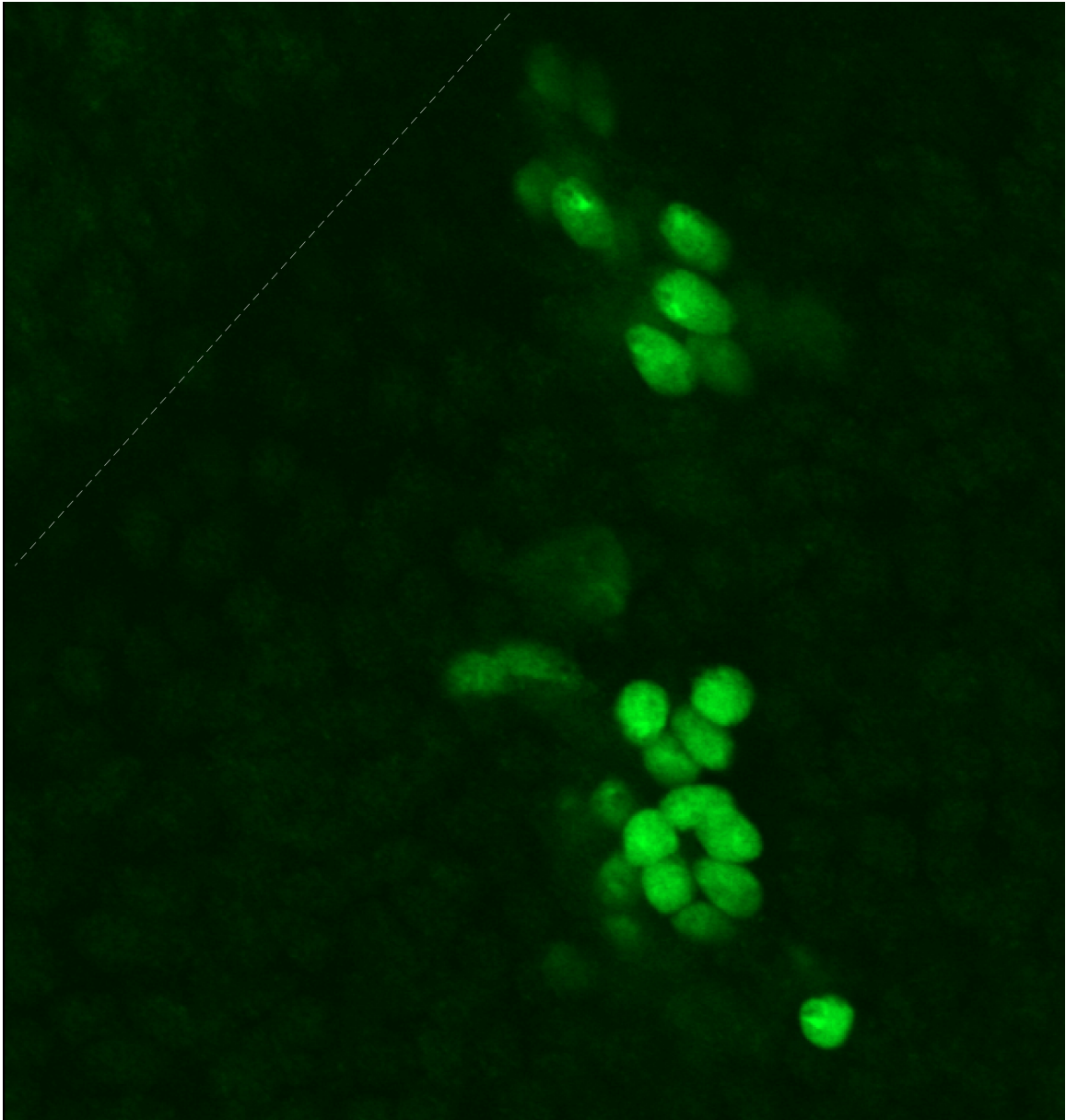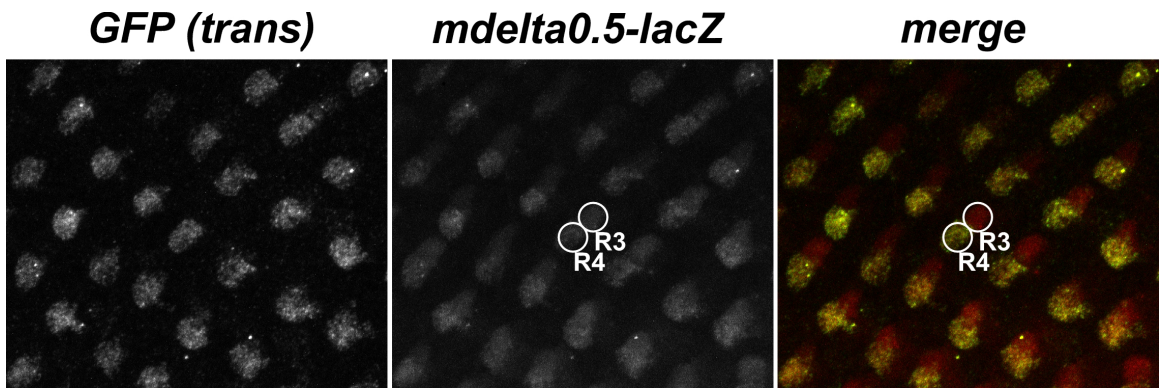Justine E. Johnson, and Jack R. Bateman

Figure S1.



100%

(20 min) GMR-hsp70-lacZ

(o/n) GMR-LTL-lacZ

2.5%

GMR-LTL-lacZ GMR-hsp70-lacZ

ey-hsp70-lacZ pax-hsp70-lacZ sal-hsp70-lacZ

Figure S2.

Figure S3.



**GFP (trans)**    **mdelta0.5-lacZ**    **merge**

Figure S4.

Figure S5.



| Enhancer | Cut:GFP overlap | Elav:GFP overlap |
|----------|-----------------|------------------|
| None | 0/19 | 23/23 |
| *aos* | 32/34 | ND |
| *pax* | 9/45 | 13/18 |

Figure S6



*pax-P+-lacZ*

*paxpaxpax-LTL-lacZ*

Figure S7.
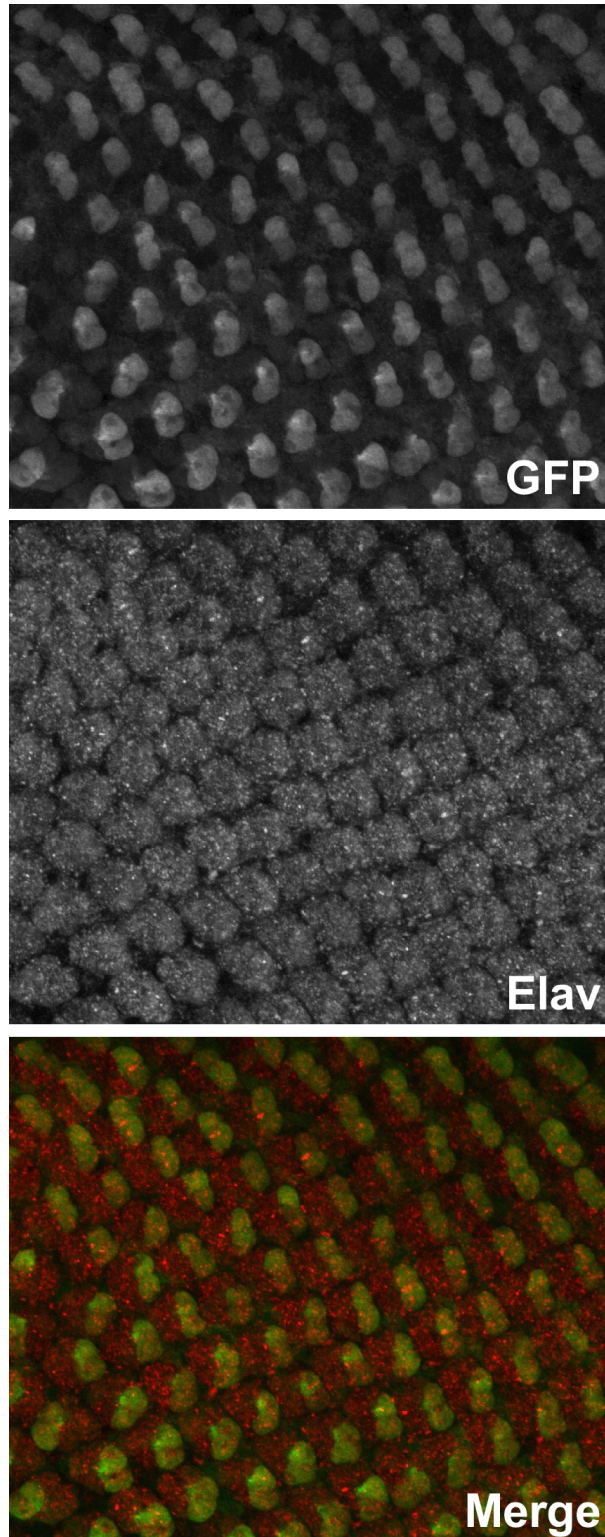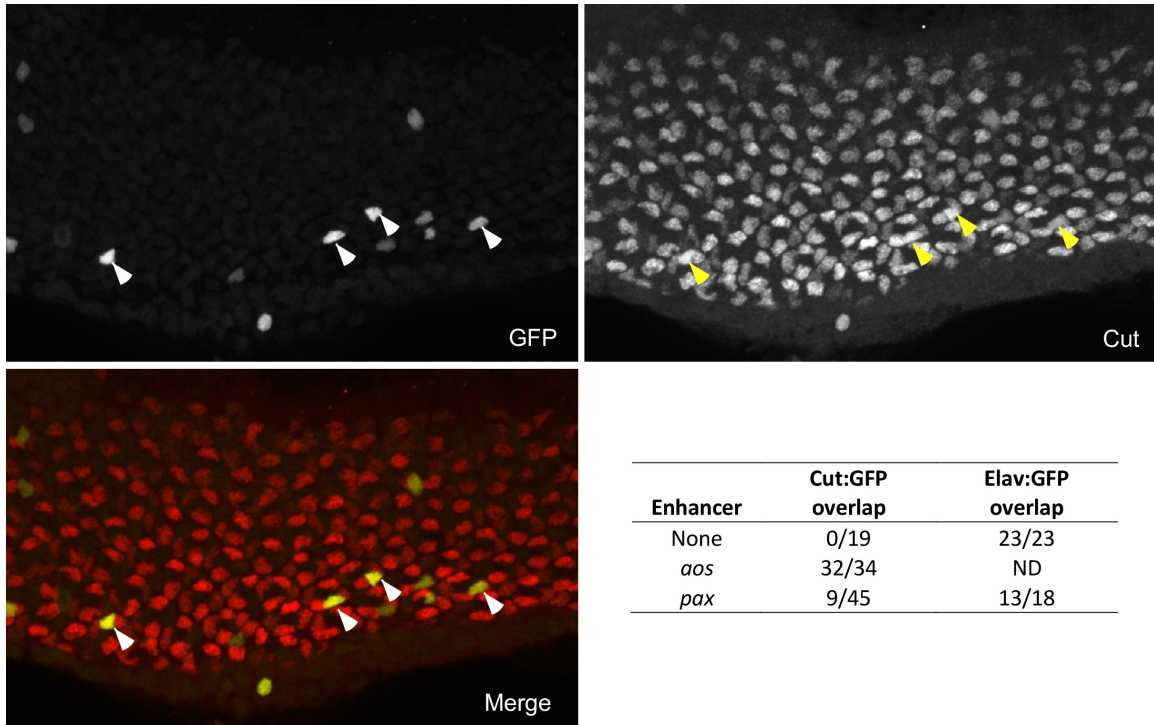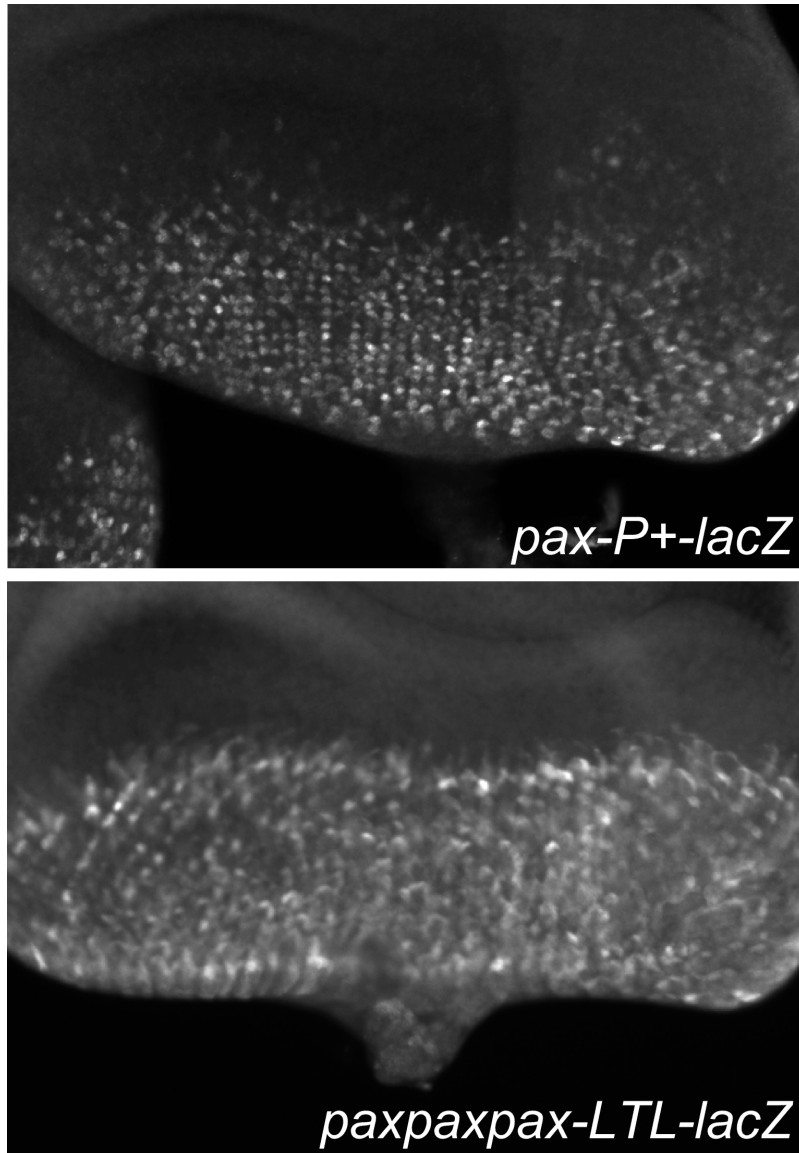


668 bp *ct* enhancer (14/14)  2.7 kb *ct* enhancer (1/10)  leaky HS-FLP (23/27)
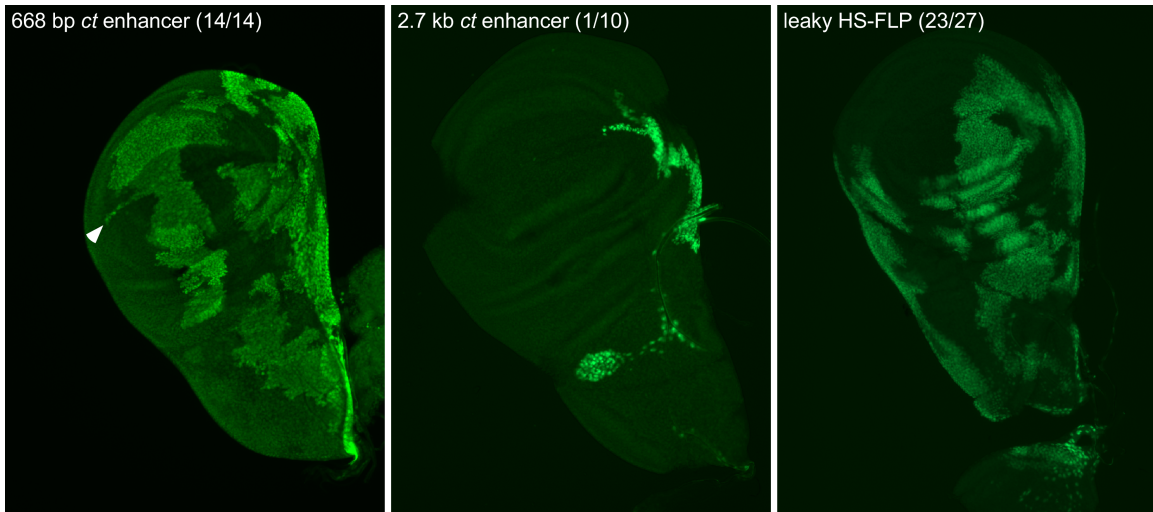
**Table S1.** Primers used to amplify enhancer fragments.

| Enhancer | Forward Primer | Reverse Primer |
|---|---|---|
| ey | CTGTTACATACTGTTCAACGAATC | AAAAGGCTAAATGGGCACAC |
| pax | GTATCAAGTAACTGGGTGCC | CCTAAGCTACCGGAAAACAA |
| CG30492 | AGGTACTAGGTTATGAGTGCTATTCCA | TGATTGTAGGTTCGAGGTTCG |
| Rh4 | ACCGAATTCCGTAATTGCTT | GTGACAGTCACCGCGATTCG |
| aos | TAACCACATCCACATCCTCA | TAGTCGGCAACATTTTGCGG |
| pros | TTCGAAATGCAGCCCAAGTT | GAGTGCAGGGGAACACGTGC |
| nmo | GCTGATGAAGCAGTGGACAA | CACCGAAAACAATGTCGAA |
| CG1625 | GCGCATTGAGTTGCGTATC | TAGCTTAGAATTAAGCACTCATTTAGA |
| Rapgap | TGCAAACTCGCTGTTTTTGA | GTGAGTCCTGCACGCATCC |
| neur | GTTGCTATCGGGCTTATGGT | TTTCGTGTGCAAGTCATTGG |
| DSCAM | GTTGGTGTCTCTGCACTGGA | AGCAAAAACCGAGGGTAAA |
| Fas2 | TGGCATCTGTTCTTTAATTTATTGTC | AAAAATAGGTAACCATCGAGTCAA |
| klu | GGATGTGGTTTTCAACGCTTGGC | AGAGGAAATGCGTAGCCTGCG |
| sev | CCAGGACGACAAGATCGAAAACAAGCA | AAAACAATATAGCAATGGCCATATAAA |
| Ser | AAGCTAAATAATCTACAATTGGGATTA | AAAAAGTAATAATGCGCCATCCGTTTG |
| ct | CATATGAATATACAATTATTGACG | AGTATGCCCATATCCC |
| sal | AGCGTGCGACAAGCATATGA | GTTCAGCCAATTTTCGGTCA |

**Table S2.** Other primers used in this study.

| Primer Name | Sequence |
|---|---|
| hsp70FLP_5_attB40 | cgggtgccagggcgtgcccTTGggctccccgggcgcgta cCGAGCGCCGGAGTATAAAT |
| hsp70FLP_3_attB40 | cgggtgccagggcgtgcccTTGggctccccgggcgcgta cGGGGGATCCAGACATGATAA |
| lac4 | ACTGTGCGTTAGGTCCTGTTCATTGT |
| 3'Pend1 | GTCGGCAAGAGACATCCACT |
| RNXG9 | GTGGTTTGTCCAAACTCATCAA |
| SV40_3'UTR_2F | GGAAAGTCCTTGGGGTCTTCTACCT |
| SV40_3'UTR_2R | TGGGAGCAGTGGTGGAATGCCT |

**Supplemental Figures**

**Figure S1. The *Lox-TATA-Lox* (*LTL*) promoter is weak relative to the minimal *hsp70* promoter.** β-galactosidase staining (upper left) and quantitative RT-PCR (upper right) show that the enhancer *GMR* activates the *LTL* promoter, an *hsp70* minimal promoter flanked by loxP sites, less efficiently than it does the *hsp70* promoter lacking loxP sites. Times indicate the length of time that the stain was allowed to develop (o/n, overnight). Quantitative RT-PCR was performed on transgenic flies that had been crossed to $w^{1118}$ to produce flies hemizygous for the insertion (upper right). PCR data represent two independent experiments. Below, β-gal staining for enhancers *ey*, *pax* (with arrowhead marking weak expression in the posterior of the eye disc), and *sal* activating *lacZ* via the *hsp70* promoter lacking loxP sites, showing expected patterns of expression for each enhancer.

**Figure S2. The *ey* enhancer acts in *trans* anterior to the morphogenetic furrow.** A single plane confocal image shows two adjacent moderate-sized clones found anterior to the morphogenetic furrow, created by activation of the G-TRACE cassette through the *ey* enhancer activating *hsp70-FLP* in trans. The disc is oriented with posterior toward the upper left; a dashed line marks the position of the furrow, which runs diagonally across the upper left of the image.

**Figure S3. *GMR* acts in *trans* primarily in photoreceptors R3 and R4.** Images show GFP fluorescence resulting from *GMR* transvection in a disc co-stained with

mδ-0.5, a marker of R4 cells (as clusters mature, the marker also appears in R3). R3 and R4 are highlighted for one ommatidial cluster. Posterior is down.

**Figure S4. GMR *cis*-expression is highest in R3 and R4.** Images show GFP fluorescence from a *GMR-hsp70-GFP* transgene in a disc co-stained for the neuronal marker Elav. Posterior is down.

**Figure S5. Transvection by the enhancers *aos* and *pax* occurs in cone cells.** Images show an example of a disc wherein transvection by the *aos* enhancer causes GFP fluorescence from a G-TRACE cassette. Co-staining of the disc with anti-Cut, a cone cell marker, shows overlap between the two channels (arrowheads). Table shows data for negative control (an enhancerless *hsp70-lacZ* in *trans* to *hsp70-FLP*; 8 discs scored for anti-Cut, 8 discs scored for anti-Elav), the *aos* enhancer (2 discs scored for anti-Cut), and the *pax* enhancer (8 discs scored for anti-Cut, 4 discs scored for anti-Elav). Two-tailed Fisher's Exact Tests comparing the cell type specificities of GFP-positive cells showed $p < 0.05$ for both enhancers relative to negative control.

**Figure S6. Multimerization of the *pax* enhancer leads to an expanded pattern of expression.** Top, a disc carrying *pax-hsp70-lacZ* (which provides more robust and consistent staining relative to *pax-LTL-lacZ*) stained with anti-β-gal, showing characteristic staining pattern for cone cell-specific expression. Bottom, a disc

carrying *paxpaxpax-LTL-lacZ* stained with anti-β-gal, showing a broader pattern of expression. See Figure 7 for detailed cell typing.

**Figure S7. *Trans*-activation of the G-TRACE system by *ct* enhancers.** The *ct(668)* enhancer consistently activates the G-TRACE transvection system (see main text) in large patches, suggesting *trans*-activation of *hsp70-FLP* very early in the development of the wing disc. In many discs, the wing margin (where *ct(668)* activity is expected) is obscured by these patches, but in some discs, activation along the wing margin is more obvious (left panel). In discs carrying the *ct(2.7)* enhancer, we have seen only one example of a small spurious patch of GFP positive cells extending from the wing margin (middle panel), with no large patches as observed with *ct(668).* However, flies carrying a leaky heat-shock *FLP* construct on the X chromosome in addition to the G-TRACE cassette show a spurious pattern of GFP positive patches (right panel) very similar to that observed with *ct(668),* suggesting that the smaller *ct* enhancer permits sporadic activation of *hsp70-FLP* in *trans* by an unknown mechanism, precluding a more comprehensive analysis of transvection by specific enhancer *trans*-activity for this construct. Fractions indicate the proportion of discs analyzed with a pattern of GFP positive cells similar to that shown; arrowhead indicates cells at the wing margin.